

Revised Version

1
2
3
4 **Complexes Based on Asymmetrically Substituted Pyridine-dithiolene Ligands**
5 **[M(4-pedt)₂] (M = Au, Cu, Ni; 4-pedt = 1-(pyrid-4-yl)-ethylene-1,2-dithiolate): Synthesis,**
6 **Structure and Physical Properties.**

7
8 Sandra Rabaça,^a Ana Cerdeira,^a Ana I.S. Neves,^a Sandra I.G Dias,^a Cécile Mézière,^b Isabel C.
9 Santos,^a Laura C.J. Pereira,^a Marc Fourmigué,^c Rui T. Henriques,^d Manuel Almeida,^a

10
11 a Departamento de Química, Instituto Tecnológico e Nuclear/CFMCUL, P-2686-953
12 Sacavém, Portugal

13 b Laboratoire CIMMA, UMR CNRS 6501, Université d'Angers, Bd. Lavoisier, F-49045
14 Angers, France

15 c Sciences Chimiques de Rennes, UMR 6226 CNRS-Université de Rennes I, Campus de
16 Beaulieu, F-35042 Rennes, France

17 d Instituto de Telecomunicações, Pólo de Lisboa, Av. Rovisco Pais 1, 1049-001 Lisboa,
18 Portugal

19
20 **Keywords:** Gold; Nickel; Copper; Dithiolene; Crystal structure; Magnetic behaviour.

21

22 **Abstract**

23 The monoanionic Ni, Au and Cu bis(dithiolene) complexes based on the
24 1-(pyridine-4-yl)-ethylene-1,2-dithiolate were prepared and isolated as $[\text{PPh}_4]^+$, $[n\text{-Bu}_4\text{N}]^+$ and
25 $[\text{Na}(\text{18c6})]^+$ salts which were characterised by single-crystal X-ray diffraction, cyclic
26 voltammetry, EPR and magnetic susceptibility measurements. All the complexes adopt a
27 square planar coordination geometry with a trans arrangement of the substituent pyridine
28 rings whose planes are rotated from 13° to 33° relatively to the central MS_4 core. The C-C and
29 C-S bond lengths are consistent with ene-1,2-dithiolate form of the ligand and M^{III} oxidation
30 state. The Ni complexes are paramagnetic with an effective magnetic moment of ~ 1.7 BM .

31

32 **Introduction**

33 Transition metal bis(dithiolene) complexes have attracted research attention for more than 30
34 years and, due to their rich redox behaviour and favourable solid state interactions in their
35 square-planar geometry, they have been widely used in the preparation of conducting and
36 magnetic materials.^[1] These complexes can be seen as inorganic analogues of the
37 corresponding TTF type donors where the transition metal replaces the central C=C bond. The
38 TTF type donors have been at the basis of the large majority of all known molecular
39 conductors and superconductors, and these inorganic analogues offer the additional advantage
40 that depending on the oxidation state and on the transition metal they can be either
41 diamagnetic or paramagnetic with different magnetic moments.

42 Recently there has been an increasing focus of attention on the preparation of donors which,
43 in addition to their electroactive role, can bind directly to transition metals and some TTF
44 derivatives substituted with groups containing N coordinating atoms^[2] and their complexes
45 have been recently described.^[3] The corresponding inorganic analogues, bis(dithiolene)

46 complexes with ligands bearing nitrogen coordinating groups have been however a lot less
47 explored. Having in mind such type of complexes, we recently focused our interest on
48 bis(dithiolene) complexes based on thio-azo ligands bearing heterocyclic groups and recently
49 described the first neutral Ni bis(dithiolene) complex (formally Ni^{IV}) with alkylpyridyl
50 substituted ligands, Ni(dpesdt)₂.^[4]

51 Asymmetrically substituted dithiolenes have been significantly less studied in spite of
52 providing also interesting properties^[5] namely for magnetic materials^[6] and optoelectronics.^[7]
53 One example of bis(dithiolene) complexes bearing heterocyclic groups are the M(*n*-pedt)₂
54 complexes (*n* = 2, 3 or 4), based on the asymmetrically substituted ligand *n*-pedt = S–
55 C(H)=C(R)–S; R = 4-pyridyl. Ligand 4-pedt was previously presented in a preliminary short
56 report^[8]. More recently monoanionic gold bisdithiolene complexes with R = *n*-pyridyl
57 ligands were also described.^[9]

58 In this paper we describe the preparation and characterization of monoanionic [M(4-pedt)₂][–]
59 complexes of nickel, copper and gold obtained as tetrabutylammonium,
60 tetraphenylphosphonium or sodium 18-crown-6 ether salts.

61

62 **2. Experimental**

63 **2.1. Materials and methods**

64 All manipulations were carried out under anaerobic conditions, unless stated otherwise.
65 Whenever required, the solvents were dried according to the standard literature procedures,^[10]
66 freshly distilled, and saturated with nitrogen prior to use. All starting reagents were purchased
67 from commercial sources and used without further purification or synthesised from published
68 methods. The 4-(4-pyridyl)-1,3-dithiol-2-one was synthesised according to literature
69 reports.^[8, 11]

70 Elemental analyses of the compounds isolated in these studies were performed at ITN
71 analytical services using an EA 110 CE Instruments automatic analyzer. Melting points were
72 performed on a Stuart Scientific SMP2.

73

74

75 **2.2. Synthesis**

76 **2.2.1. Tetraphenylphosphonium salt of bis[1-(4-pyridyl)-1,2-ethylenedithiolato]nickel,**

77 **PPh₄ [Ni(4-pedt)₂] (1):** The 4-(4-pyridyl)-1,3-dithiol-2-one (0.50 g, 2.56 mmol) was added to
78 a sodium methanolate solution (0.147 g; 6.40 mmol; 13 mL) After 45 minutes of stirring,
79 Ni(NO₃).6H₂O (0.37 g, 1.28 mmol) was added. One hour later the red solution was filtered to
80 an aqueous PPh₄Cl solution (0.96 g, 2.56 mmol, 100 mL). A black precipitate appeared
81 immediately from the brown solution. The solid was recovered by filtration, washed with
82 water and recrystallised from acetonitrile to afford black crystals of the nickel salt suitable for
83 X-ray diffraction. 50% yield (0.47 g, 0.64 mmol); m.p. 217-218 °C. C₃₈H₃₀NiN₂PS₄ (Mol.
84 Wt.: 732.59). Elemental Anal. Calc.: C 62.30; H 4.13; N 3.82; S 17.51%. Found: C 62.09;
85 H 4.06; N 3.77; S 17.31%.

86

87 **2.2.2. Tetraphenylphosphonium salt of bis[1-(4-pyridyl)-1,2-ethylenedithiolato]copper**

88 **PPh₄ [Cu(4-pedt)₂] (2):** The oxo compound (0.10 g; 0.51 mmol) was added to a freshly made
89 sodium methoxide solution (0.023 g; 1.02 mmol, 3 mL) and stirred at room temperature, until
90 total dissolution, followed by drop wise addition of a solution of CuCl₂.2H₂O (0.043 g;
91 0.25 mmol) in methanol (2 mL). The solution was stirred for one hour and filtered into a
92 PPh₄Br methanol solution (0.214 g, 0.51 mmol, 3 mL). No precipitate formation was
93 observed. The reaction vial was opened to the air, a few H₂O drops were slowly added until

94 start of incipient precipitation and the mixture was left overnight at 4°C. The oil that formed
95 was separated from the mixture by centrifugation, dried under vacuum (P₂O₅) and
96 recrystallised from dichloromethane/hexane to be recovered as a microcrystalline precipitate.
97 48% yield (0.089 g, 0.12 mmol); m.p. 162-163 °C. C₃₈H₃₀N₂CuS₄ (Mol. Wt.:737.44).
98 Elemental Anal. Calc.: C, 61.89; H, 4.10; N, 3.80; S, 17.39%. Found: C, 61.72; H, 4.92; N,
99 3.84; S, 18.03%.

100

101 **2.2.3. Tetrabutylammonium salt of bis[1-(4-pyridyl)-1,2-ethylenedithiolato]nickel**

102 ***n*-Bu₄N [Ni(4-pedt)₂] (3):** The procedure was similar to the described above. The oxo
103 compound was added (0.10 g; 0.51 mmol) to a freshly made sodium methoxide solution
104 (0.023 g; 1.02 mmol, 3 mL) and stirred at room temperature, until total dissolution, followed
105 by drop wise addition of a solution of NiCl₂.6H₂O (0.061 g; 0.25 mmol) in methanol (2 mL).
106 The red solution was stirred for one hour and then filtered into *n*-Bu₄NBr methanol solution
107 (0.165 g, 0.51 mmol, 3 mL). No precipitate formation was observed. The reaction vial was
108 opened to the air, a few H₂O drops were slowly added until start of incipient precipitation and
109 the mixture was left overnight at 4 °C. The reddish oil formed was separated from the mixture
110 by centrifugation, dried under vacuum (P₂O₅) and recrystallised from acetone to be recovered
111 as a microcrystalline precipitate. 65% yield (0.105 g, 0.16 mmol); m.p. 133-134 °C.
112 C₃₀H₄₆N₃NiS₄ (Mol. Wt.: 635.66) Elemental Anal. Calc.: C, 56.68; H, 7.29; N, 6.61;
113 S, 20.18%. Found: C, 56.01; H, 7.89; N, 6.12; S, 19.75%.

114

115 **2.2.4. Tetrabutylammonium salt of bis[1-(4-pyridyl)-1,2-ethylenedithiolato]copper,**

116 ***n*-Bu₄N [Cu(4-pedt)₂] (4):** Following the same general procedure used for
117 *n*-Bu₄N[Ni(4-pedt)₂]. The oxo compound was added (0.10 g; 0.51 mmol) to a freshly made
118 sodium methoxide (0.023 g; 1.02 mmol, 3 mL) stirred until total dissolution, followed by drop

119 wise addition of a solution of $\text{CuCl}_2 \cdot 2\text{H}_2\text{O}$ (0.043 g; 0.25 mmol) in methanol (2 mL). The
120 solution was stirred for one hour and afterwards filtered onto an *n*- Bu_4NBr methanol solution
121 (0.165 g, 0.51 mmol, 3 mL). No precipitate formation was observed. A few H_2O drops were
122 slowly added until start of incipient precipitation and the mixture was left overnight at 4 °C.
123 The oil formed was separated from the mixture by centrifugation, dried under vacuum (P_2O_5)
124 and recrystallised from dichloromethane/hexane to be recovered as a microcrystalline
125 precipitate. 41% yield (0.065g, 0.10 mmol); m.p. 160-162 °C. $\text{C}_{30}\text{H}_{46}\text{N}_3\text{CuS}_4$ (Mol. Wt.:
126 640.51) Elemental Anal. Calc.: C, 56.26; H, 7.24; N, 6.56; S, 20.02%. Found: C, 55.83; H,
127 7.01; N, 6.12; S, 19.84%.

128

129 **2.2.5. Tetrabutylammonium salt of bis[1-(4-pyridyl)-1,2-ethylenedithiolato]gold**
130 ***n*- Bu_4N [$\text{Au}(4\text{-pedt})_2$] (5):** Following the same general procedure used for
131 *n*- Bu_4N [$\text{Ni}(4\text{-pedt})_2$], the oxo compound (0.10 g; 0.51 mmol) was dissolved in a freshly
132 prepared methoxide solution (0.024 mg; 1.02 mmol, 3 mL). The total dissolution of the oxo
133 compound was followed by drop wise addition of a $\text{KAuCl}_4 \cdot 4\text{H}_2\text{O}$ methanol solution
134 (0.097 g; 0.25 mmol, 2 mL). The brown solution was filtered into an *n*- Bu_4NBr methanol
135 solution (0.165 g, 0.51 mmol, 3 mL). After the addition of a few milliliters of water, the
136 reaction vial was left for several hours at 4 °C. The brown oil formed was recovered by
137 centrifugation, dried under vacuum (P_2O_5) and recrystallised from dichloromethane/hexane to
138 be recovered as a microcrystalline precipitate. 60% yield (0.115 g, 0.15 mmol); m.p. 127-
139 129 °C. $\text{C}_{30}\text{H}_{46}\text{N}_3\text{AuS}_4$ (Mol. Wt.: 773.93). Elemental Anal. Calc: C, 46.56; H, 5.99; N, 5.43;
140 S, 16.57%. Found: C, 46.21; H, 5.52; N, 5.25; S, 16.39%.

141

142 **2.2.6. Crown ether [Na(18c6)] salt of bis[1-(4-pyridyl)-1,2-ethylenedithiolato]nickel**
143 **[Na(18c6)] [$\text{Ni}(4\text{-pedt})_2$], (6):** The oxo compound (0.20 g; 1.03 mmol) was added to a freshly

144 prepared methoxide solution (0.047 g, 2.05 mmol, 5 mL). After stirring until total dissolution,
145 NiCl₂.6H₂O methanol solution (0.122 g; 0.51 mmol, 5 mL) was added. The red solution was
146 stirred for one hour and then filtered into an 18c6 methanol solution (0.271 g, 1.03 mmol,
147 1 mL). The mixture was left at 4 °C for two weeks. A mixture of amorphous brown and
148 darker polycrystalline precipitate was recovered by vacuum filtration. The mixture was
149 dissolved in dichloromethane and an insoluble precipitate was removed. By slow diffusion of
150 hexane into the dichloromethane solution, it was possible to recover compound **6** as a dark
151 brown polycrystalline material. Yield 0.197 g, 0.29 mmol (58%); m.p. 260-
152 261. C₂₆H₃₄N₂NaNiO₆S₄ (Mol.Wt. 680.5)°C. Elemental Anal. . Calc. C 45.89; H 5.04; N 4.12;
153 S 18.85%. Found: C 45.43; H 5.35; N 4.12; S 18.30%.

154

155 **2.2.7.Crown ether [Na(18c6)] salt of bis[1-(4-pyridyl)-1,2-ethylenedithiolato] gold**
156 **[Na(18c6)] [Au(4-pedt)₂], (7):** The oxo compound (0.10 g, 0.51 mmol) was added to a
157 freshly prepared sodium methoxide solution (0.0235 g, 1.02 mmol, 5 ml) and stirred for 45
158 minutes. The dark red solution was removed from the inert atmosphere and solid
159 KAuCl₄.4H₂O (0.097 g, 0.25 mmol) was added. The mixture was stirred for 2 hours, filtered
160 over Celite to a solution of 18c6 (0.0677 g, 0.25 mmol) in methanol (1 ml) and layered with
161 pentane and left at 4 °C. A few days later, an amorphous brown precipitate was recovered by
162 vacuum filtration. From an attempt to recrystallise from dichloromethane/hexane, an oil was
163 obtained which was dried and characterised. Yield 0.088 g, 0.11 mmol (44%); m.p. 145-146
164 °C. C₂₆H₃₄O₆N₂S₄AuNa (Mol.Wt. 818.08). Elemental Anal. Calc : C 38.14, H 4.19, N 3.42,
165 S 15.63%. Found: C 38.38, H 4.91, N 3.50, S 15.28%.

166

167

168

169 **2.3. Physical characterization**

170 Cyclic voltammetry data were obtained using a BAS C3 Cell Stand. The measurements were
171 performed at room temperature in CH₂Cl₂ solutions, containing [*n*-Bu₄] PF₆ (0.1M) as
172 supporting electrolyte, with a scan rate of 100 mV/s using platinum wire working and counter
173 electrodes and a Ag/AgCl reference electrode. The [(Me₅C₅)₂Fe]⁺/[(Me₅C₅)₂Fe] ([Fc*]⁺/[Fc*])
174 couple was used as the internal reference and the potentials of the redox couples observed
175 were referenced to that.

176 Single crystals suitable for X-ray crystallographic analyses were obtained by recrystallisation
177 in acetonitrile, for compound **1**, and by slow diffusion of hexane into a saturated solution of
178 dichloromethane, for compounds **2**, **3**, **5** and **6**. In compound **6** two water molecules were
179 incorporated in the crystal structure to yield compound **6·2H₂O**, due to the presence of air
180 humidity

181 The data for compounds **1**, **2**, **3**, **5** and **6a** were collected on a Bruker AXS APEX CCD area
182 detector X-ray diffractometer equipped with an Oxford Cryosystems low-temperature device
183 at 150 K in the ω and φ scans mode. A semi empirical absorption correction was carried out
184 using SADABS.^[12] Data collection, cell refinement and data reduction were done with the
185 SMART and SAINT programs.^[13] The structures were solved by direct methods using
186 SIR97^[14] and refined by fullmatrix least-squares methods with the SHELXL97^[15] program
187 using the winGX software package.^[16] Non-hydrogen atoms were refined with anisotropic
188 thermal parameters whereas H-atoms were placed in idealised positions and allowed to refine
189 riding on the parent C atom. In **3** and **5** one of the butyl groups on the cation show disorder
190 that was modelled over two positions with the following occupation factors: 52%:48% and
191 55%:45% respectively. The final difference Fourier map revealed the existence of residual
192 electron densities of: 2.4/-0.89 eÅ⁻³ for compound **5**, which are located near the Au atom.

193 Molecular graphics were prepared using ORTEP3^[17] and Mercury 1.4.2.^[18] A summary of the
194 crystal data, structure solution and refinement is listed in Table 1.

195

196

197 Table 1 - Crystallographic data and refinement parameters for complexes $\text{Ph}_4\text{P}[\text{Ni}(4\text{-pedt})_2]$ (**1**), $\text{Ph}_4\text{P}[\text{Cu}(4\text{-pedt})_2]$ (**2**), $n\text{-Bu}_4\text{N}[\text{Ni}(4\text{-pedt})_2]$ (**3**),
 198 $n\text{-Bu}_4\text{N}[\text{Au}(4\text{-pedt})_2]$ (**5**) and $[\text{Na}(18\text{c6})][\text{Ni}(4\text{-pedt})_2]\cdot 2\text{H}_2\text{O}$ (**6·2H₂O**).

Compound	1	2	3	5	6·2H₂O
Formula	$\text{C}_{38}\text{H}_{30}\text{N}_2\text{NiP}\text{S}_4$	$\text{C}_{38}\text{H}_{30}\text{CuN}_2\text{P}\text{S}_4$	$\text{C}_{30}\text{H}_{46}\text{N}_3\text{Ni}\text{S}_4$	$\text{C}_{30}\text{H}_{46}\text{AuN}_3\text{S}_4$	$\text{C}_{26}\text{H}_{38}\text{N}_2\text{NaNiO}_8\text{S}_4$
Formula weight (g mol ⁻¹)	732.58	737.39	635.65	773.90	712.49
Wavelength (Å)	0.71073	0.71073	0.71073	0.71073	0.71073
Crystal system, Space group	Monoclinic, <i>C2/c</i>	Monoclinic, <i>C2/c</i>	Triclinic, <i>P-1</i>	Triclinic, <i>P-1</i>	Monoclinic, <i>P2₁/n</i>
<i>a</i> (Å)	26.8750(5)	26.9179(8)	9.0033(2)	8.6211(1)	11.7067(14)
<i>b</i> (Å)	17.3528(3)	17.3541(6)	11.2258(2)	11.1196(2)	9.7243(12)
<i>c</i> (Å)	18.1609(3)	18.1969(5)	16.9070(3)	17.6962(3)	14.3179(18)
α (°)	90	90	107.7870(10)	74.646(1)	90
β (°)	127.5650(10)	127.3820(10)	90.3960(10)	88.829(1)	96.103(2)
γ (°)	90	90	98.3450(10)	80.336(1)	90
<i>V</i> (Å ³), <i>Z</i>	6713.4(2), 8	6754.5(4), 8	1607.48(5), 2	1612.14(4), 2	1620.7(3), 2
ρ_{calc} (Mg/m ³), μ (mm ⁻¹)	1.450, 0.906	1.450, 0.973	1.313, 0.887	1.594, 4.846	1.468, 0.918
<i>F</i> (000)	3032	3040	678	780	750
Crystal size (mm)	0.4 x 0.3 x 0.08	0.30 x 0.20 x 0.16	0.28 x 0.24 x 0.20	0.38 x 0.30 x 0.28	0.20 x 0.12 x 0.10
θ Range (°)	2.83 to 25.03	2.74 to 25.68	3.21 to 25.35	2.64 to 25.68	2.73 to 25.68
Collected <i>hkl</i>	-31 ≤ <i>h</i> ≤ 31 -20 ≤ <i>k</i> ≤ 20 -21 ≤ <i>l</i> ≤ 21	-32 ≤ <i>h</i> ≤ 32 -21 ≤ <i>k</i> ≤ 21 -20 ≤ <i>l</i> ≤ 22	-10 ≤ <i>h</i> ≤ 10 -13 ≤ <i>k</i> ≤ 13 -20 ≤ <i>l</i> ≤ 20	-10 ≤ <i>h</i> ≤ 10 -13 ≤ <i>k</i> ≤ 13 -21 ≤ <i>l</i> ≤ 21	-14 ≤ <i>h</i> ≤ 12 -11 ≤ <i>k</i> ≤ 11 -17 ≤ <i>l</i> ≤ 17
Reflections collected	41666	23618	13680	17908	7273
Independent reflections	5910 [R(int) = 0.0424]	6409 [R(int) = 0.0656]	5821 [R(int) = 0.0422]	6122 [R(int) = 0.0306]	3051 [R(int) = 0.0414]
Completeness to θ	25.03 99.7 %	25.68 99.7 %	25.35 98.9 %	25.68 99.7 %	25.68 99.3 %
Absorption correction	Semi-empirical from equivalents				
Max. and min. transmission	0.8052 and 0.7133	0.8599 and 0.7590	0.8425 and 0.7893	0.3440 and 0.2603	0.9139 and 0.8378
Refinement method	Full-matrix least-squares on <i>F</i> ²				
Data / restraints / parameters	5910 / 0 / 418	6409 / 0 / 418	5821 / 6 / 370	6122 / 2 / 370	3051 / 2 / 201
Goodness-of-fit on <i>F</i> ²	1.069	1.049	1.079	1.071	1.035
Final <i>R</i> indices [<i>I</i> > 2 σ (<i>I</i>)]	<i>R</i> ₁ = 0.0276, <i>wR</i> ₂ = 0.0711	<i>R</i> ₁ = 0.0396, <i>wR</i> ₂ = 0.0868	<i>R</i> ₁ = 0.0366, <i>wR</i> ₂ = 0.0899	<i>R</i> ₁ = 0.0254, <i>wR</i> ₂ = 0.0590	<i>R</i> ₁ = 0.0376, <i>wR</i> ₂ = 0.0791
<i>R</i> indices (all data)	<i>R</i> ₁ = 0.0341, <i>wR</i> ₂ = 0.0740	<i>R</i> ₁ = 0.0644, <i>wR</i> ₂ = 0.0945	<i>R</i> ₁ = 0.0482, <i>wR</i> ₂ = 0.0947	<i>R</i> ₁ = 0.0401, <i>wR</i> ₂ = 0.0630	<i>R</i> ₁ = 0.0659, <i>wR</i> ₂ = 0.0853
Larg. diff. peak and hole (e Å ⁻³)	0.416 and -0.355	0.422 and -0.473	0.556 and -0.280	2.348 and -0.895	0.392 and -0.502

200 EPR spectra were obtained at room temperature on powders using a conventional X-band
201 spectrometer (Bruker ESP 300 E) equipped with a microwave bridge ER041XK, a rectangular
202 cavity operating in T102 mode and a field controller ER 032M system. The modulation
203 amplitude was kept well below the linewidth and the microwave power well below saturation.
204 Static magnetic susceptibility measurements in the range 2-300 K were performed using a
205 superconducting longitudinal Faraday system (Oxford Instruments) under a magnetic field of
206 5 T and field gradient of 1 T/m. A polycrystalline sample (~20 mg) was placed inside a
207 previous calibrated thin-wall Teflon bucket. The force was measured with a microbalance
208 (Sartorius S3D-V), applying forward and reverse field gradients. Magnetisation data were
209 corrected for contributions due to the sample holder and core diamagnetism, estimated from
210 tabulated Pascal constants as -385×10^{-6} , -379×10^{-6} and -348×10^{-6} emu/mol for **1**, **3** and **6**
211 respectively.

212

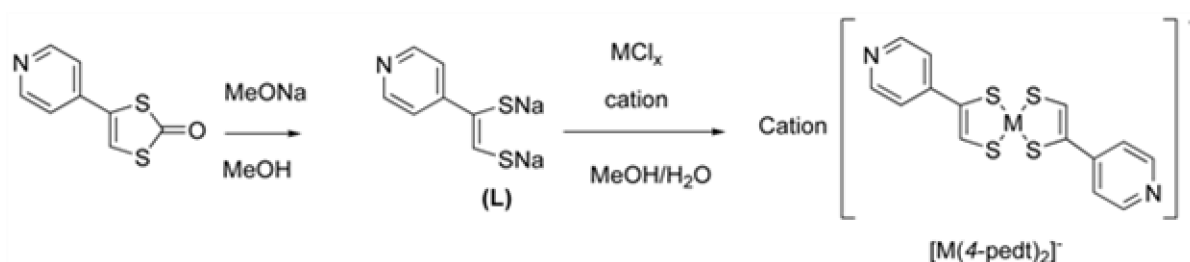
213 **3. Results and Discussion**

214 **3.1. Synthesis**

215 The synthesis of the nickel, copper and gold complexes **1** to **7** were performed following
216 standard procedures for this type of dithiolene ligands (Scheme 1). The dithiolate ligand (**L**)
217 was obtained from the corresponding oxo compound by hydrolytic cleavage with sodium
218 methoxide and without intermediate isolation it was reacted with the selected metal salt to
219 give an anionic complex which is precipitated as a salt in the presence of the selected cation.
220 The presence of water was needed to precipitate the dithiolene complex from the solution. In
221 case of **1**, a water solution of the cation was added and the dithiolene complex precipitated
222 immediately as a black precipitate. In the case of compounds **2**, **3**, **4** and **5** a few drops of
223 water were added at the end of the reaction until the start of incipient precipitation and after

224 keeping the reaction mixture at 4 °C it was possible to collect the product as fine precipitate
 225 which tends to form an oil. Compounds **6** and **7** were obtained without adding water after
 226 keeping the solution a few days at 4 °C until complexes precipitated. These complexes were
 227 obtained after recrystallisation from acetonitrile, acetone or dichloromethane/hexane in
 228 overall yields between 41 and 65%.

229 Complexes **1-7** were characterised by elemental analyses and cyclic voltammetry studies. The
 230 elemental analyses after the recrystallisations are consistent with a 1:1 cation:anion
 231 stoichiometry, in agreement with the X-ray crystal structure determination of the diffracting
 232 single crystals. While this is expected for $M = \text{Au}$, for Cu and Ni even though starting from a
 233 $\text{Ni}^{\text{II}}\text{Cl}_2$ or $\text{Cu}^{\text{II}}\text{Cl}_2$ salt, the dianionic dithiolene complexes could not be obtained, even under
 234 nitrogen atmosphere and the monoanionic dithiolene complexes were obtained as evidenced
 235 by the X-ray structure determination or by the electronic paramagnetic resonance (EPR)
 236 spectroscopy. Whereas complexes **1**, **2**, **3**, **5** and **6·2H₂O** were unambiguously characterised
 237 by single X-ray structure determination, compounds **4**, **6** and **7** could not be studied by single
 238 X-ray diffraction due to their poor crystal quality.



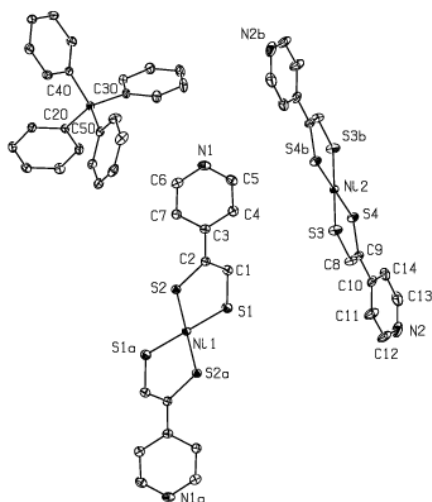
239 $(\text{Ph}_4\text{P})[\text{Ni}(\text{4-pedt})_2]$ (**1**) $\eta=50\%$; $(\text{Ph}_4\text{P})[\text{Cu}(\text{4-pedt})_2]$ (**2**) $\eta=48\%$; $(n\text{-Bu}_4\text{N})[\text{Ni}(\text{4-pedt})_2]$ (**3**) $\eta=65\%$; $(n\text{-Bu}_4\text{N})[\text{Cu}(\text{4-pedt})_2]$ (**4**) $\eta=41\%$;
 $(n\text{-Bu}_4\text{N})[\text{Au}(\text{4-pedt})_2]$ (**5**) $\eta=60\%$; $[\text{Na}(\text{18c6})][\text{Ni}(\text{4-pedt})_2]$ (**6**) $\eta=58\%$; $[\text{Na}(\text{18c6})][\text{Au}(\text{4-pedt})_2]$ (**7**) $\eta=44\%$

240
 241
 242

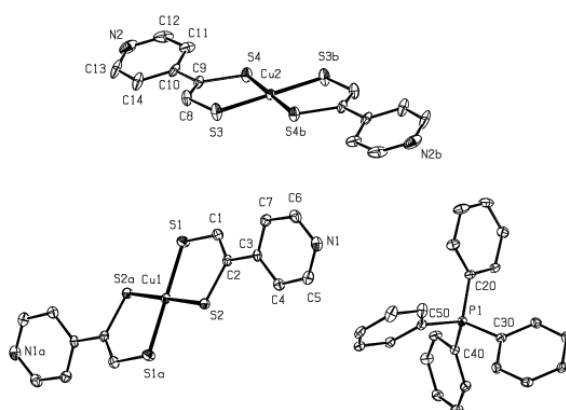
Scheme 1

243 **3.2. Crystal Structure**

244 Compounds **1**, **2**, **3**, **5** and **6·2H₂O** have been characterised by single crystal X-ray diffraction
245 technique. The ORTEP views of these compounds are shown in Figs. 1-5. Selected bond
246 angles and distances are given in Table 2.

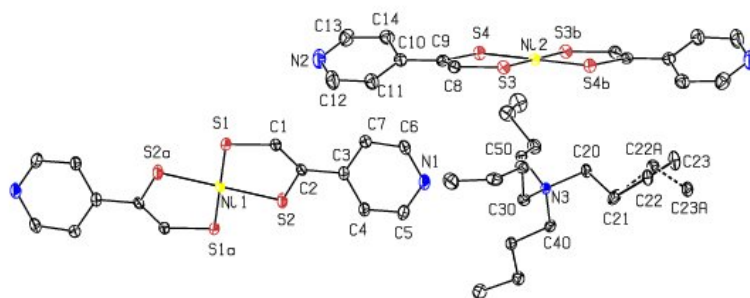


247
248 Figure 1. Ortep views of the cation and the two independent anion units of Ph₄P [Ni(4-pedt)₂],
249 (**1**), showing the atomic numbering scheme. Displacement ellipsoids are drawn at the 30%
250 probability level. H atoms have been omitted for clarity. [Symmetry codes: (a) 2-x, 1-y, 1-z;
251 (b) 1.5-x, 1.5-y, 1-z].

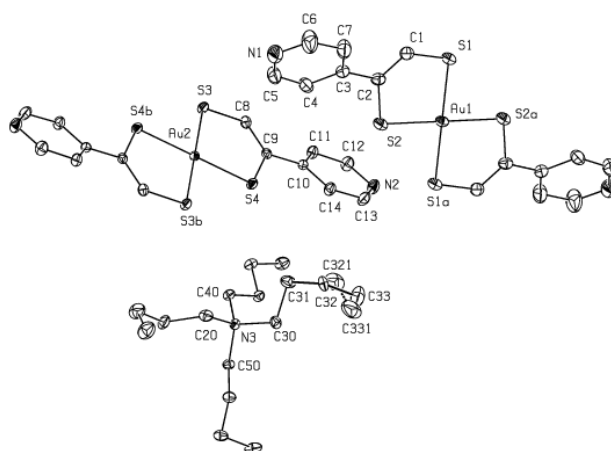


252
253 Figure 2. Ortep views of the cation and the two independent anion units of
254 Ph₄P [Cu(4-pedt)₂], (**2**), showing the atomic numbering scheme. Displacement ellipsoids are

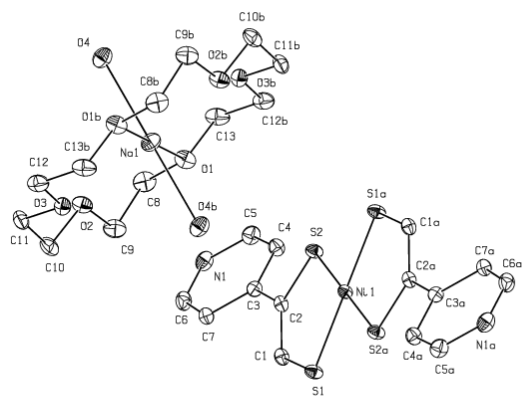
255 drawn at the 30% probability level. H atoms have been omitted for clarity. [Symmetry codes:
256 (a) 1-x, 1-y, z; (b) 0.5-x, 1.5-y, -z].



257
258 Figure 3. Ortep views of the cation and the two independent anion units of
259 *n*-Bu₄N [Ni(4-pedt)₂], (**3**), showing the atomic numbering scheme. Displacement ellipsoids
260 are drawn at the 30% probability level. H atoms have been omitted for clarity. [Symmetry
261 codes: (a) -x, -y, -z; (b) 1-x, 1-y, 1-z].



262
263 Figure 4. Ortep views of the cation and the two independent anion units of
264 *n*-Bu₄N [Au(4-pedt)₂], (**5**), showing the atomic numbering scheme. Displacement ellipsoids
265 are drawn at the 30% probability level. H atoms have been omitted for clarity. [Symmetry
266 codes: (a) -x, -y, -z; (b) 1-x, 1-y, 1-z].



267

268 Figure 5. Ortep views of the cation and anion units of $[\text{Na}(18\text{c}6)] [\text{Ni}(4\text{-pedt})_2] \cdot 2\text{H}_2\text{O}$,
 269 $(6 \cdot 2\text{H}_2\text{O})$, showing the atomic numbering scheme. Displacement ellipsoids are drawn at the
 270 30% probability level. H atoms have been omitted for clarity. [Symmetry codes: (a) $-x, -y, -z$;
 271 (b) $2-x, 1-y, 1-z$].

272

273 The monoanionic Ph_4P salts **1** and **2** are isostructural and crystallise in the monoclinic system,
 274 space group $C2/c$, $Z = 8$, the asymmetric unit comprising one cation $[\text{PPh}_4]^+$ located in a
 275 general position and two independent half-anions $[\text{M}(4\text{-pedt})_2]^-$; ($\text{M} = \text{Ni}$ and Cu for
 276 compound **1** and **2**, respectively) both with the metals located at an inversion centre. The
 277 angle between the two $[\text{M}(4\text{-pedt})_2]^-$ units mean planes is about 49.47° and 49.52° for
 278 compound **1** and **2** respectively.

279 The monoanionic $n\text{-Bu}_4\text{N}$ salts **3** and **5** are isostructural and crystallise in the triclinic system,
 280 $P-1$ space group, $Z = 2$. The asymmetric unit comprising two independent half-anion units;
 281 both the metal atoms located at inversion centres and with one cation unit located at a general
 282 position. The angle between the anionic units mean planes is about 88.98° and 89.81° for **3**
 283 and **5** respectively.

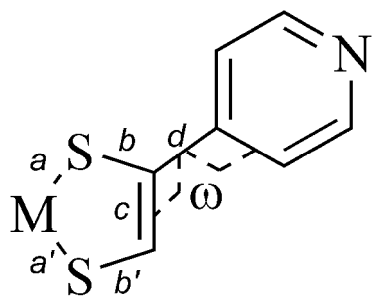
284 The compound **6·2H₂O** crystallises in the monoclinic system, space group $P2_1/n$, $Z = 2$. The
285 asymmetric unit comprises one independent half-anion unit and one independent half-cation
286 unit located at inversion centres.

287 In all complexes, the centrosymmetric anion $[M(4\text{-pedt})_2]^-$ ($M = \text{Ni, Cu or Au}$) adopts a
288 square-planar coordination geometry and a *trans* conformation. The central core of the anions,
289 constituted by the metal atom, the four sulphur atoms and the four carbon atoms, is essentially
290 planar (rms deviation of fitted atoms are 0.0091 Å and 0.0057 Å for compound **1**; 0.0182 and
291 0.0237 Å for compound **2**, 0.0152 Å and 0.0268 Å for compound **3**; 0.0537 Å and 0.0250 Å
292 for compound **5**; 0.0125 Å for compound **6·2H₂O**).

293

294

295 Table 2 - Important bond lengths (in Å) within the metallocycle, the torsion angle ω (in °) between the pyridine group plane and the metallocycle
 296 plane and δ -parameter (defined below) for compounds **1**, **2**, **3**, **5** and **6·2H₂O**.



297

Compound	1	3	6·2H₂O	2	5				
	M = Ni ₂	M = Ni ₁	M = Ni ₁	M = Ni ₂	M = Ni	M = Cu ₁	M = Cu ₂	M = Au ₂	M = Au ₁
M-S (<i>a</i>)	2.1293(5)	2.1507(5)	2.1383(5)	2.1549(6)	2.1375(7)	2.1871(7)	2.1626(7)	2.3078(10)	2.3183(13)
M-S (<i>a'</i>)	2.1474(5)	2.1416(5)	2.1463(6)	2.1478(7)	2.1531(7)	2.1797(8)	2.1812(8)	2.3053(11)	2.3082(11)
S-C (<i>b</i>)	1.737(2)	1.742(2)	1.739(2)	1.740(3)	1.738(3)	1.771(3)	1.765(3)	1.768(4)	1.771(4)
S-C (<i>b'</i>)	1.715(2)	1.715(2)	1.713(2)	1.715(2)	1.714(3)	1.735(3)	1.740(3)	1.742(4)	1.735(5)
C=C (<i>c</i>)	1.353(3)	1.351(3)	1.364(3)	1.351(3)	1.354(4)	1.335(4)	1.328(4)	1.345(6)	1.336(6)
C-C (<i>d</i>)	1.478(3)	1.476(3)	1.474(3)	1.476(3)	1.469(4)	1.481(4)	1.483(4)	1.477(5)	1.476(7)
ω	13.14(6)	28.50(8)	29.51(8)	28.64(7)	33.56(7)	28.92(12)	13.90(8)	21.83(13)	33.44(17)
δ	1.26	1.55	1.49	1.44	1.38	2.03	1.42	1.47	2.03

298 $\delta = 100(b-b')/b$

299

300

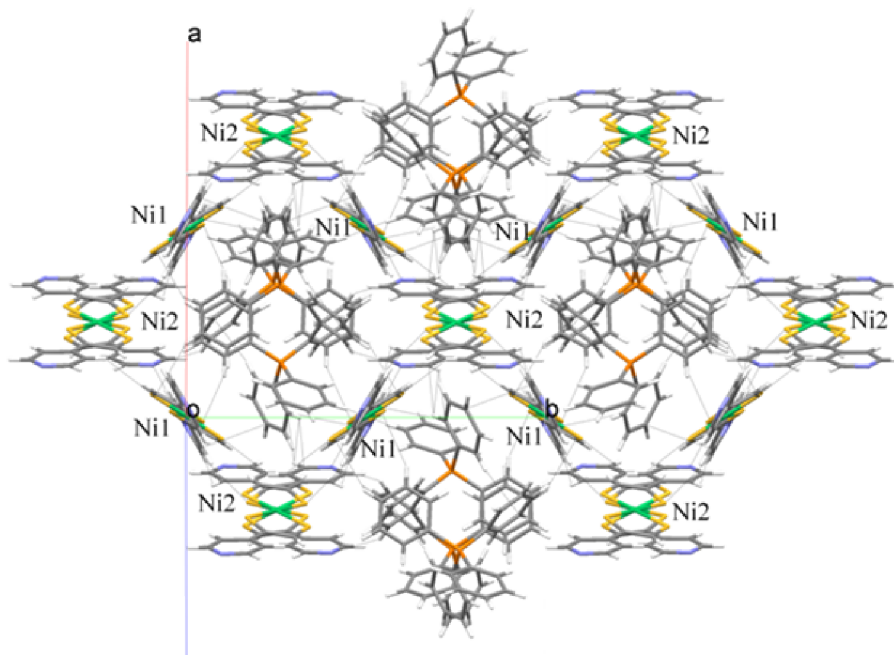
301 Important bond lengths within the MS_2C_2 metallocycle are collected in Table 2. The average
302 M-S bond lengths are in good agreement with values found in other Ni, Cu and Au
303 monoanionic dithiolate complexes, respectively.^[1c),19,20,21] While the central core of the
304 complexes is planar, the two pyridine rings are rotated out of the central core plane with
305 dihedral angles between 13° and 33° depending on the complex, with the majority of them
306 between 21° and 33° , only one of the anionic units in the Ph_4P salts **1** and **2** presents a smaller
307 angle of about 13° . The rotation of the pyridine rings is induced by steric hindrance between
308 hydrogen atoms at the 2-position of the pyridine ring and in the metallocycle carbon but this
309 rotation is also assisted by the interaction with neighbouring molecular units in the solid. The
310 salts **5** and **6·2H₂O** present the higher pyridine rotation values ($\sim 33^\circ$) and this large value can
311 be ascribed to cation interactions (and also anion interactions in the case of complex **5**) as
312 denoted by several short contacts (see tables SM1-SM2 and figures SM1 SM2).

313 The smaller pyridine rotations of only $\sim 13^\circ$, in **1** and **2**, are associated with anionic and
314 cationic interactions, including π - π interactions between the pyridine groups of the
315 $[M(4\text{-pedt})_2]^-$ units: (see tables SM3-SM4 and figure SM3). The two pyridine rings involved
316 are coplanar with distances close to the sum of the Van der Waals radii, clearly denoting
317 significant π - π interactions (Figure SM3 c).

318 A feature related to the unsymmetrical nature of the 4-pedt ligand, is the S-C bond length
319 difference within the metallocycle (Table 2). The shortening of the **b'** bond when compared
320 with the **b** bond can be evaluated in terms of a parameter $\delta = 100(b-b')/b$, as previously done
321 on other unsymmetrical bis-dithiolene complexes as the $[Ni(\text{adt})_2]^-$ (adt = acrylonitrile-1,2-
322 dithiolate) or the $[Ni(\text{tfadt})_2]^-$ (tfadt = 2-(trifluoromethyl)acrylonitrile-1,2-dithiolate).^[6, 22] In
323 our case δ values are between 1.26 and 2.03% in the four structures analysed and it can be
324 attributed to the mesomeric effect of the pyridine group.

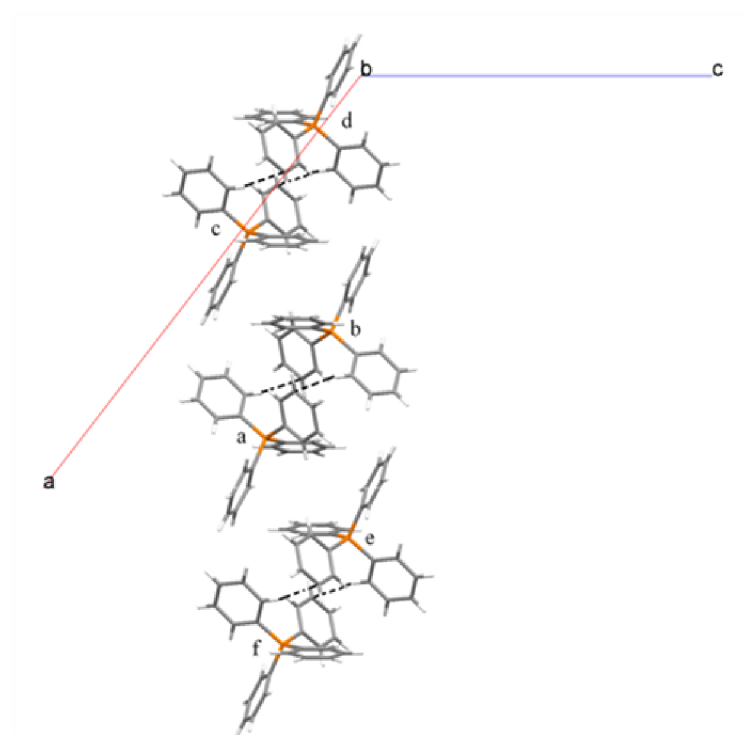
325 A long debated aspect of the dithiolene complexes is the so called “non-innocence” of the
326 ligands, which may lead to formal ambiguities in the description of the different oxidation
327 states of these complexes.^[19] In these monoanionic complexes the, ligand may have a
328 significant contribution to the frontier orbitals and can be viewed as being present in one of
329 two extreme forms: the dianionic ene-1,2-dithiolate or the neutral dithioketone.^[1a,19] In this
330 particular case of the $[M(4\text{-pedt})_2]^-$ dithiolenes where the dithiole ring is not fused to any
331 aromatic ring the lengths of the C–C and C–S bonds provide a direct indication on the nature
332 of a dithiolene ligand. In all complexes studied the C=C (1.32-1.36 Å) and C-S (1.71-1.77 Å)
333 bond lengths were found in the range typical of sp^2 C hybridisation^[23] indicative of the ene-
334 1,2-dithiolate form of the dithiolene and M(III) oxidation state. In the solid state, the
335 monoanionic $[M(4\text{-pedt})_2]^-$ species with M = Ni, Cu and Au, present different packing
336 patterns and interactions depending on the cation type complexes. The compounds **1** and **2** are
337 isostructural with the previously reported $[PPh_4]^+[Au(4\text{-pedt})_2]^-$.^[9] A characteristic of their
338 crystal structure is the occurrence of cation columns along $b+c$, isolated by a alveolar anion
339 arrangement (Figure 6). As **1** and **2** are isostructural, we will only focus our structural analysis
340 on the compound **1**. In the cation column, it is possible to observe cation pairs and the only
341 intra column short contact is H25 \cdots C54 (2.785(3) Å) (Figure 7). Such inversion-centred
342 arrangements of PPh_4^+ cations are a recurrent feature among molecules bearing at least three
343 phenyl rings on the same atoms.^[24] In the alveolar anionic arrangement there are no S-S short
344 contacts, but there are several other N \cdots H, S \cdots H, H \cdots H short contacts and π - π interactions
345 (Table SM3). Of particular note are the C52-H52 \cdots N2 (3.514(4) Å) and C6-H6 \cdots N2
346 (3.537(3) Å) weak hydrogen bonding interactions.

347



348

349 Figure 6. Crystal structure of **1**, viewed along the cation stacking axis.



350

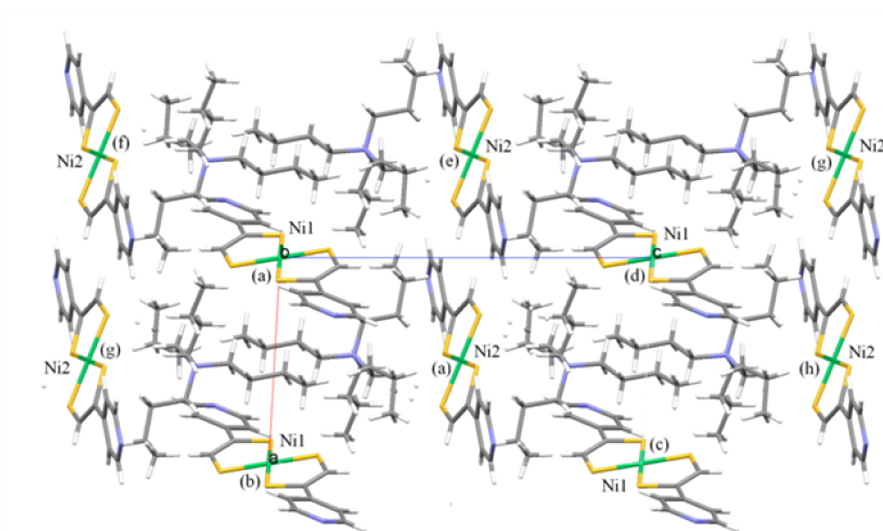
351 Figure 7. Chain of $[\text{PPh}_4]^+$ cations in compound **1** viewed along b . [Symmetry codes: (a) $x, y,$

352 z ; (b) $1.5-x, \frac{1}{2}-y, 1-z$; (c) $-\frac{1}{2}+x, \frac{1}{2}-y; -\frac{1}{2}+z$; (d) $1-x, y, \frac{1}{2}-z$; (e) $2-x, y, 1.5-z$; (f) $\frac{1}{2}+x,$

353 $\frac{1}{2}-y, \frac{1}{2}+z$].

354

355 The crystal structure of the two tetrabutylammonium salts (**3** and **5**) can be seen as made from
356 parallel mixed chains constituted by pairs of cations alternating with an anion. The parallel
357 chains alternate with sheets of anions (Figure 8). These two compounds have several short
358 intermolecular contacts but none of them corresponds to S-S interactions. (for compound **5**
359 Table SM1).

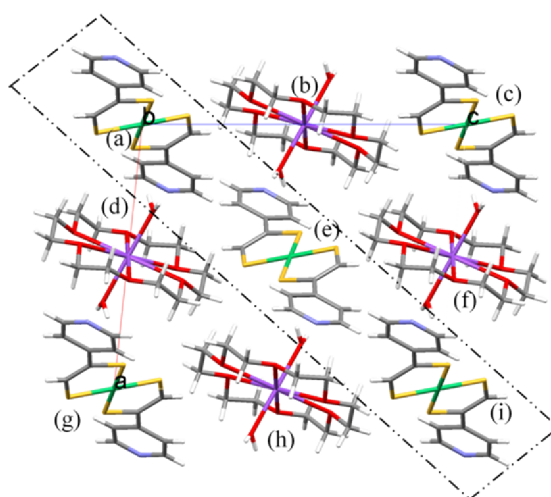


360

361 Figure 8. Crystal structure of **3**, viewed along the *b* axis. [Symmetry codes: (a) x, y, z ; (b)
362 $1+x, y, z$; (c) $1+x, 1+y, 1+z$; (d) $x, 1+y, 1+z$; (e) $-1+x, y, z$; (f) $-1+x, -1+y, -1+z$, (g) $x, -1+y,$
363 $-1+z$, (h) $x, 1+y, 1+z$, (i) $-1+x, 1+y, 1+z$].

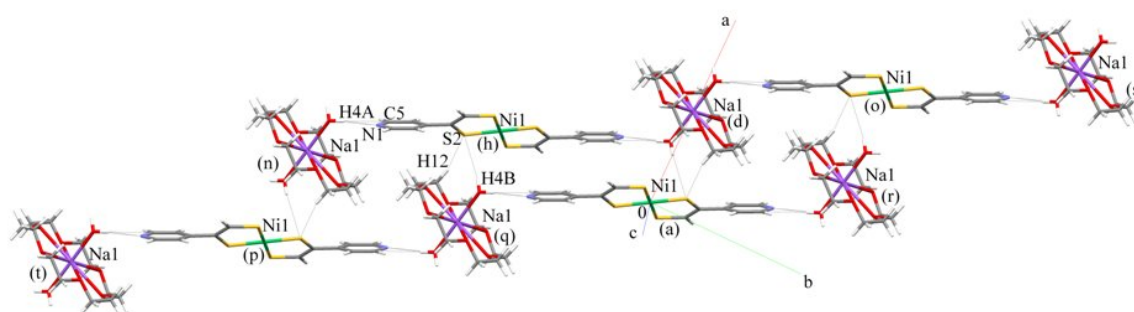
364

365 The crystal structure of compound **6·2H₂O** can be described in terms of parallel alternated
366 layers of $[\text{Ni}(4\text{-pedt})_2]^-$ anions and $\text{Na}(18\text{c}6)^+$ cations. The coordination sphere of the sodium
367 cation is completed by two water molecules, one on each side (Figure 9). The angle between
368 the anionic units mean plan is about 44.53° . Only between anions and cations, there are
369 relevant interactions. Besides several $\text{N}\cdots\text{O}$, $\text{N}\cdots\text{H}$, $\text{C}\cdots\text{H}$, $\text{O}\cdots\text{S}$, $\text{S}\cdots\text{H}$ short contacts a hydrogen
370 bond $\text{N1}\cdots\text{H4A-O4}$ ($2.916(4)$ Å) is present, which is the most important, governing the chain-
371 like arrangement anion-cation-anion(...) as depicted in Figure 10.



372

373 Figure 9. Crystal structure of $6 \cdot 2\text{H}_2\text{O}$, viewed along the b axis. The dashed box marks a layer
 374 of $[\text{Ni}(4\text{-pedt})_2]^-$ anions. [Symmetry codes: (a) x, y, z ; (b) $-1+x, y, z$, (c) $x, y, 1+z$, (d) $1.5-x, -$
 375 $1/2+y, 1/2-z$, (e) $1/2-x, 1/2+y, 1/2-z$, (f) $1.5-x, -1/2+y, 1.5-z$, (g) $1+x, y, z$, (h) $x, -1+y, z$, (i)
 376 $1+x, y, 1+z$].



377

378 Figure 10. Detail of the mixed layer in $6 \cdot 2\text{H}_2\text{O}$, two adjacent mixed chains. [Symmetry codes:
 379 (a) x, y, z ; (d) $1.5-x, -1/2+y, 1/2-z$, (n) $1/2-x, -2.5+y, 1/2-z$, (o) $1+x, 1+y, z$, (p) $-1+x, -2+y, z$,
 380 (q) $1/2-x, -1.5+y, 1/2-z$, (r) $1.5-x, 1/2+y, 1/2-z$, (s) $2.5-x, 1.5+y, 1/2-z$, (t) $-1/2-x, -3.5+y, 1/2-z$].

381

382 3.3. Redox behaviour

383 The redox behaviour of the different complexes was studied by cyclic voltammetry in CH_2Cl_2
 384 solution containing $[n\text{-Bu}_4\text{N}] \text{PF}_6$ (0.1 M) as electrolyte. Each of the compounds **1**, **3** and **6**

385 containing the Ni complex (cyclic voltammogram of compound **6**, Supplementary material,
386 Figure 4 SM) exhibit two quasi reversible redox waves, at circa -0.52 V and 0.30 V vs.
387 [Fc]⁺/[Fc] which are ascribed to the couples [Ni(4-pedt)₂]²⁻/[Ni(4-pedt)₂]⁻ and [Ni(4-pedt)₂]⁻
388 /[Ni(4-pedt)₂]⁰ (Table 3). The E^{1/2} potentials for the Ni complexes in these three compounds
389 are, identical. The variation in the scan rate (from 10 to 200mVs⁻¹) monitoring the wave
390 profile, the separation of the peak potentials (ΔE>59mV), and the ratio of the cathodic and
391 anodic currents (-I_p^c/I_p^a ≈ 1) indicate that the processes are quasi reversible. The low values of
392 the first process explain the difficulty in preparing the dianionic complex, which can be
393 spontaneously oxidised by minor amounts of oxygen or other oxidising agents. On the other
394 hand the low value of the second process predicts that the neutral complex can be prepared.
395 However attempts to isolate it were so far not successful.

396 The compounds **2** and **4** containing the Cu complex (cyclic voltammogram of compound **2**,
397 Supplementary material, Figure 5 SM) show also identical cyclic voltammograms with one
398 quasi reversible redox process at ca -0.38 V, ascribed to the couples [Cu(4-pedt)₂]²⁻/[Cu(4-
399 pedt)₂]⁻ (Table 3). Scans to higher positive potentials (~0.6V vs. vs. [Fc]⁺/[Fc]) reveal the
400 existence of an irreversible process which should correspond to the couple [Cu(4-pedt)₂]⁻
401 /[Cu(4-pedt)₂]⁰.

402 The compounds **5** and **7** containing the [Au(4-pedt)₂]⁻ complex (cyclic voltammogram of
403 compound **7**, Supplementary material, Figure 6 SM) both exhibit one oxidation and a
404 reduction process, assigned to the couples [Au(4-pedt)₂]⁻/[Au(4-pedt)₂]⁰ (Table 3). For both
405 gold compounds, the E^{1/2} potentials are very similar. A variation in the scan rate (from 10 to
406 200mVs⁻¹) monitoring the wave profile, the separation of the peak potentials (ΔE>59mV), and
407 the ratio of the cathodic and anodic currents (-I_p^c/I_p^a ≠ 1) indicate that the oxidation is not
408 electrochemically reversible.

410 Table 3. Redox potentials (mV, vs. $[\text{Fc}]^+ / [\text{Fc}]$) of **1-6** at room temperature in CH_2Cl_2
 411 containing $[n\text{-Bu}_4\text{N}] \text{PF}_6$ (0.1 M) with a 100 mVs^{-1} scan rate.

Compound	$[\text{ML}_2]^{2-} / [\text{ML}_2]^-$	$[\text{ML}_2]^- / [\text{ML}_2]^0$
$[n\text{-Ph}_4\text{P}][\text{Ni}(4\text{-pedt})_2]$ (1)	-519	297
$[n\text{-Ph}_4\text{P}][\text{Cu}(4\text{-pedt})_2]$ (2)	-374	676
$[n\text{-Bu}_4\text{N}][\text{Ni}(4\text{-pedt})_2]$ (3)	-523	303
$[n\text{-Bu}_4\text{N}][\text{Cu}(4\text{-pedt})_2]$ (4)	-379	771
$[n\text{-Bu}_4\text{N}][\text{Au}(4\text{-pedt})_2]$ (5)		585
$[\text{Na}(18\text{c}6)][\text{Ni}(4\text{-pedt})_2]$ (6)	-518	298
$[\text{Na}(18\text{c}6)][\text{Au}(4\text{-pedt})_2]$ (7)		588

412

413 It is known that the nature of the R substituent in the complexes $\text{Ni}(\text{S}_2\text{C}_2\text{R}_2)_2$ affects the redox
 414 potentials and even a small variation in the electron withdrawing substituent can tune the
 415 redox potential.^[1a, 25] In this case we observe that the pyridine groups, which are only partially
 416 rotated relatively to the central bisdithiolene plane, thus retaining the possibility of interacting
 417 via their pi systems, make the 4-pedt complexes easier to oxidize than phenyl substituted or
 418 even unsubstituted edt ligands.^[5]

419

420 3.4. EPR measurements

421 While the monoanionic Cu and Au complexes are diamagnetic the monoanionic Ni,
 422 complexes, as d^7 system in a square planar coordination are expected to be paramagnetic
 423 $S = 1/2$ systems. Indeed the EPR spectra of **1**, **3** and **6**, as powders, show a signal typical of
 424 monoanionic Ni dithiolene complexes^[1,26,27] with rhombic symmetry, with $g_1 = 2.1035$,
 425 $g_2 = 2.0518$, $g_3 = 2.0128$ for the compound **1** and $g_1 = 2.1153$, $g_2 = 2.0480$, $g_3 = 2.0087$ for the
 426 compound **6**. In the case of the compound **3** the EPR spectrum denotes the existence of two

427 Ni sites with different g_1 (2.0849 and 2.0834) and g_3 (2.0183 and 2.0113) values but with the
428 same (or very close) g_2 value (2.0701). This should be related with the different
429 crystallographic environments of the two anionic Ni units in the asymmetric unit of the
430 compound **3**. In fact Ni1 unit besides quite asymmetric Ni-S bonds lengths has several short
431 S...H-C contacts with cations which are absent in unit Ni2. In spite of the existence of two
432 different anionic Ni^{III} units in the asymmetric unit of **1**, the two sets of g principal values for
433 this compound are not distinguishable within experimental error in agreement with the fact
434 that the two Ni units present comparable short contacts between the S atoms.

435

436 **3.5. Magnetic susceptibility**

437 The magnetic susceptibility measurements of the compounds **1** and **3** in the range 2-300 K
438 indicate a paramagnetic behaviour with effective magnetic moments essentially temperature
439 independent down to ~15 K with values at room temperature of 1.72 and 1.79 respectively.
440 For compound **6**, the room temperature magnetic moment is 1.67 BM, but it slightly increases
441 upon cooling down to 11 K (1.85 BM), denoting weak ferromagnetic interactions, that are not
442 effective at lower temperature (confirmed by magnetisation vs. magnetic field at 3.1 K – see
443 Supplementary material). These values are consistent with a $S = 1/2$ state, due to an unpaired
444 electron of a d^7 system in an quadrangular coordinating geometry. The calculated magnetic
445 moment for the three compounds assuming a Curie law for $S = 1/2$ and g values g_{av} from EPR
446 is 1.78 BM.

447

448 **Conclusion,**

449 The new paramagnetic complex, $[\text{Ni}(4\text{-pedt})_2]^-$, with the dithio-azo 4-pedt ligand has been
450 synthesised, and isolated as the $[\text{PPh}_4]^+$, $[n\text{-Bu}_4\text{N}]^+$ and $\text{Na}^+(18\text{c6})$ salts, which were

451 characterised by single crystal X-ray diffraction, cyclic voltametry EPR and magnetic
452 susceptibility. These three compounds present three distinct crystal structures and similar
453 magnetic and redox behaviour, characteristic of monoanionic Ni complexes with
454 quadrangular coordinating geometry and exhibit two quasi reversible redox waves, attributed
455 to the $[\text{Ni}(4\text{-pedt})_2]^{2-} / [\text{Ni}(4\text{-pedt})_2]^-$ and $[\text{Ni}(4\text{-pedt})_2]^- / [\text{Ni}(4\text{-pedt})_2]^0$ redox processes.

456 Two other complexes with the same dithio-azo ligand have been synthesised, $[\text{Au}(4\text{-pedt})_2]^-$
457 and $[\text{Cu}(4\text{-pedt})_2]^-$, isolated as the $[n\text{-Bu}_4\text{N}]^+$ and $\text{Na}^+(18\text{c}6)$ salts in case Au and as the
458 $[\text{PPh}_4]^+$, $[n\text{-Bu}_4\text{N}]^+$ salts in case Cu, all them exhibiting diamagnetic behaviour.

459 The $[n\text{-Bu}_4\text{N}]^+$ and $[\text{PPh}_4]^+$ salts of Au and Cu complexes are isostructural with the
460 correspondent Ni ones. Both Ni and Cu complexes present a similar quasi reversible redox
461 process corresponding to the couple $[\text{ML}_2]^{2-} / [\text{ML}_2]^-$ but they differ in the couple $[\text{ML}_2]^-$
462 $/ [\text{ML}_2]^0$ which is a quasi reversible process for Ni and an irreversible one for Cu. For the Au
463 complexes only the couple $[\text{ML}_2]^- / [\text{ML}_2]^0$ is observed.

464 The ability of the pyridine groups of these complexes to coordinate other metals is presently
465 under study and will be reported subsequently.

466

467 **Appendix A. Supplementary material**

468 CCDC 698755, 698756, 698757, 698758 and 698759 contain the supplementary
469 crystallographic data **1**, **2**, **3**, **5** and **6.2H₂O**. These data can be obtained free of charge via
470 <http://www.ccdc.cam.ac.uk/conts/retrieving.html>, or from the Cambridge Crystallographic
471 Data Centre, 12 Union Road, Cambridge CB2 1EZ, UK; fax: (+44) 1223-336-033; or e-mail:
472 deposit@ccdc.cam.ac.uk. Supplementary data associated with this article can be found, in the
473 online version.

474

475 **Acknowledgements,**

476 This work was partially supported by FCT trough contract (PTDC/QUI/64967/2006) and by
477 GRICES-Ministère des Affaires Etrangères (France) Pessoa n° 07981RL bilateral agreement
478 and it also benefited from the ESF COST action D35.

479

480 **References**

[1] a) J. A. McCleverty, *Prog. Inorg. Chem.* 10 (1968) 49-221. b) D. Coucouvanis, *Prog. Inorg. Chem.* 11 (1970) 233-371. c) R. Eisenberg, *Prog. Inorg. Chem.* 12 (1970) 295-369. d) L. Alcácer, H. Novais, *Extended Linear Chain Compounds*, Vol. 3 (Ed.: J. S. Miller), chapter 6, p. 319, Plenum Press, New York, 1983. e) S. Alvarez, R. Vicente, R. Hoffmann, *J. Am. Chem. Soc.* 107 (1985), 6253-6277. f) T. B. Rauchfuss, *Prog. Inorg. Chem.* 52 (2004) 1-54 g) N. Robertson, L. Cronin, *Coord. Chem. Rev.* 227 (2002) 93-127.

[2] a) N. Bendellat, Y. Le Gal, S. Golhen, A. Gouasmina, L. Ouahab, J. M. Fabre, *Eur. J. Inorg. Chem.* (2006) 4237–4241; b) J. D. Wallis, J. P. Griffiths, *J. Mat. Chem.* 15 (2005) 347–365.

[3] a) Y. Xu, D. Zhang, H. Li, D. Zhu, *J. Mat. Chem.* 9 (1999) 1245–1249. b) F. Iwarhori, S. Golhen, L. Ouahab, R. Carlier, J.-P. Sutter, *Inorg. Chem.* 40 (2001) 6541–6542. c) F. Setifi, L. Ouahab, S. Golhen, Y. Yoshida, G. Saito, *Inorg. Chem.* 42 (2003) 1791–1793. d) A. Ota, L. Ouahab, S. Golhen, O. Cador, Y. Yoshida, G. Saito, *New J. Chem.* 29 (2005) 1135–1140. e) L. Wang, B. Zhang, J. Zangh, *Inorg. Chem.* 45 (2006) 6860–6863. f) M. Chahma, N. Hassan, A. Alberola, H. Stoeckli-Evans, M. Pilkington, *Inorg. Chem.* 46 (2007) 3807–3809. g) M. Moshimann, S.-X. Liu, G. Labat, A. Neels, S. Decurtins, *Inorg. Chimica Acta* 360 (2007) 3848–3854. h) Q. Zhu, Y. Lu, Y. Zhang, G. K. Bian, G.-Y. Niu, J. Dai, *Inorg. Chem.*

46 (2007) 10065–10070. i) S. I. G. Dias, A. I. S. Neves, S. Rabaça, I. C. Santos, M. Almeida, *Eur. J. Inorg. Chem.* (2008) 4728–4734.

[4] S. Rabaça, M. C. Duarte, I. C. Santos, M. Fourmigué, M. Almeida, *Inorg. Chim. Acta*, 360 (2007) 3797-3801.

[5] V. Madhu, S. K. Das, *Inorg. Chem.* 47 (2008) 5055-5070.

[6] a) M. Fourmigué, J. N. Bertran, *Chem. Comm.* (2000) 2111-2112, b) L. N. Dawe, J. Miglioi, L. Turnbow, M. L. Taliaferro, W. W. Shum, J. D. Bagnato, L. V. Zakharov, A. L. Rheingold, A.M. Arif, M. Fourmigué, J. S. Miller, *Inorg. Chem.* 44 (2005) 7530-7539.

[7] S. Shi (D. M. Roundhill, J. P. Fackler, Jr. Eds), *Optoelectronic Properties of Inorganic Compounds*, 52-153, Plenum, New York, 1999.

[8] E. Cerrada, J. Garrido, M. Laguna, N. Lardiés, I. Romeo, *Synthetic Metals* 102 (1999) 1709-1710.

[9] J. M. Tunney, A. J. Blake, E. S. Davies, J. McMaster, C. Wilson, C. D. Garner, *Polyhedron* 25 (2006) 591-598.

[10] D. D. Perrin, W. L. F. Armarego, *Purification of Laboratory Chemicals*, Pergamon, Oxford, 1988.

[11] O. P. Levi, J. Y. Becker, A. Ellern, V. Khodorkovsky, *Tetrahedron Lett.* 42 (2001) 1571-73.

[12] G. M. Sheldrick, SADABS, Bruker AXS Inc., Madison, Wisconsin, USA, 2004.

[13] Bruker. SMART and SAINT, .Bruker AXS Inc., Madison, Wisconsin, USA, 2004.

[14] A. Altomare, M. C. Burla, M. Camalli, G. Cascarano, G. Giacovazzo, A. Guagliardi, A. G. G. Moliterni, G. Polidori, R. Spagna, *J. Appl. Cryst.* 32 (1999) 115.

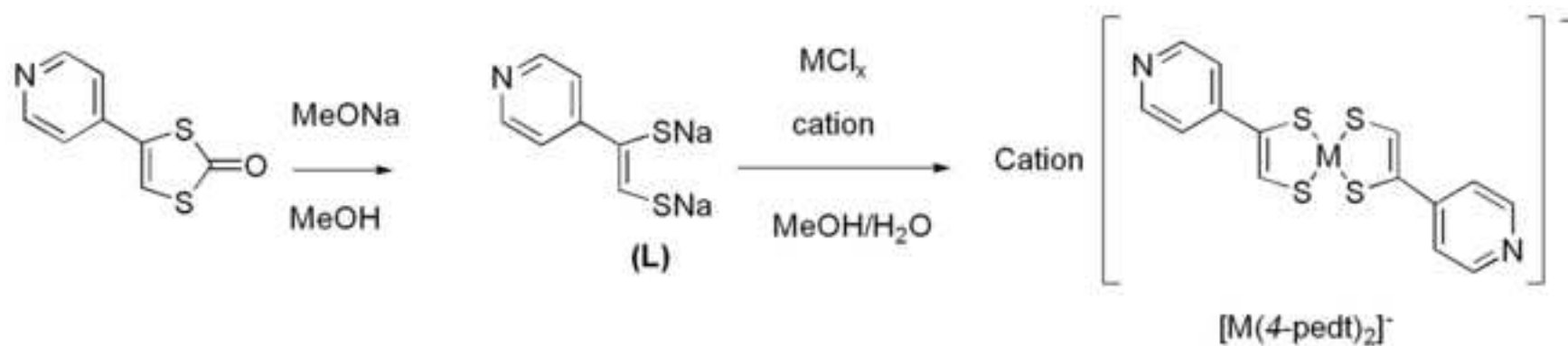
[15] G.M. Sheldrick, SHELXL97, Program for Crystal Structure Refinement, University of Goettingen, Germany, 1997.

[16] L. J. Farrugia, *J. Appl. Cryst.* 32 (1999) 837-838.

-
- [17] L. J. Farrugia, *J. Appl. Cryst.* 30 (1997) 565.
- [18] Mercury: visualization and analysis of crystal structures, C. F. Macrae, P. R. Edgington, P. McCabe, E. Pidcock, G. P. Shields, R. Taylor, M. Towler, J. van de Streek, *J. Appl. Cryst.* 39 (2006) 453-457.
- [19] B. S. Lim, D. V. Fomitchev, R. H. Holm, *Inorg. Chem.* 40 (2001) 4257-4262.
- [20] K. Ray, T. Weyhermüller, A. Goossens, M. W. J. Crajé, K. Wieghardt, *Inorg. Chem.* 42 (2003) 4082-4087.
- [21] a) H. Alves, D. Simão, H. Alves, D. Belo, S. Rabaça, E. B. Lopes, V. Gama, M. T. Duarte, R. T. Henriques, H. Novais, M. Almeida, *Eur. J. Inorg. Chem.* (2001) 3119-3126 ; b) H. Alves, D. Simão, I. C. Santos, V. Gama, R. T. Henriques, H. Novais, M. Almeida, *Eur. J. Inorg. Chem.* (2004) 1318-1329 ; c) E. B. Lopes, H. Alves, I. C. Santos, D. Graf, J. S. Brooks, E. Canadell, M. Almeida, *J. Mat. Chem.* 18 (2008) 2825–2832.
- [22] O. Jeannin, J. Delaunay, F. Barrière, M. Fourmigué, *Inorg. Chem.* 44 (2005) 9763-9770.
- [23] F.H. Allen, O. Kennard, D.G. Watson, *J. Chem. Soc. Perkin Trans. II* (1987) S1-S19.
- [24] I. Dance, M. Scudder, *Chem. Eur. J.* 2 (1996) 481-486.
- [25] a) D. C. Olson, V. P. Mayweg, G. N. Schrauzer, *J. Am. Chem. Soc.* 86 (1966) 4876-4882; b) E. Hoyer, *Chemistry and Industry*, 10 (1965) 652-653.
- [26] a) A. Davison, N. Edelstein, R. H. Holm, A. H. Maki, *Inorg. Chem.* 2 (1963) 1227-1232; b) D. Belo, H. Alves, S. Rabaça, L. C. Pereira, M. T. Duarte, V. Gama, R. T. Henriques, M. Almeida, E. Ribera, C. Rovira, J. Veciana, *Eur. J. Inorg. Chem.* (2001) 3127-3133.
- [27] a) R.P. Burns, C.A. McAuliffe, *Adv. Inorg. Chem. Radiochem.* 22 (1979) 303-348; b) R. Kirmse, J. Stach, W. Dietzsch, G. Steimecke, E. Hoyer, *Inorg. Chem.* 19 (1980) 2679-2685; R. Kirmse, J. Stach, U. Abram, W. Dietzsch, B. Bottcher, M.C.M. Gribnau, C.P. Keijzers, *Inorg. Chem.* 23 (1984) 3333-3338.

Scheme1

[Click here to download high resolution image](#)



$(\text{Ph}_4\text{P})[\text{Ni}(4\text{-pedt})_2]$ (**1**) 50% yield; $(\text{Ph}_4\text{P})[\text{Cu}(4\text{-pedt})_2]$ (**2**) 48% yield; $(n\text{-Bu}_4\text{N})[\text{Ni}(4\text{-pedt})_2]$ (**3**) 65% yield; $(n\text{-Bu}_4\text{N})[\text{Cu}(4\text{-pedt})_2]$ (**4**) 41% yield;
 $(n\text{-Bu}_4\text{N})[\text{Au}(4\text{-pedt})_2]$ (**5**) 60% yield; $[\text{Na}(18\text{c}6)][\text{Ni}(4\text{-pedt})_2]$ (**6**) 58% yield; $[\text{Na}(18\text{c}6)][\text{Au}(4\text{-pedt})_2]$ (**7**) 44% yield

Figure 1

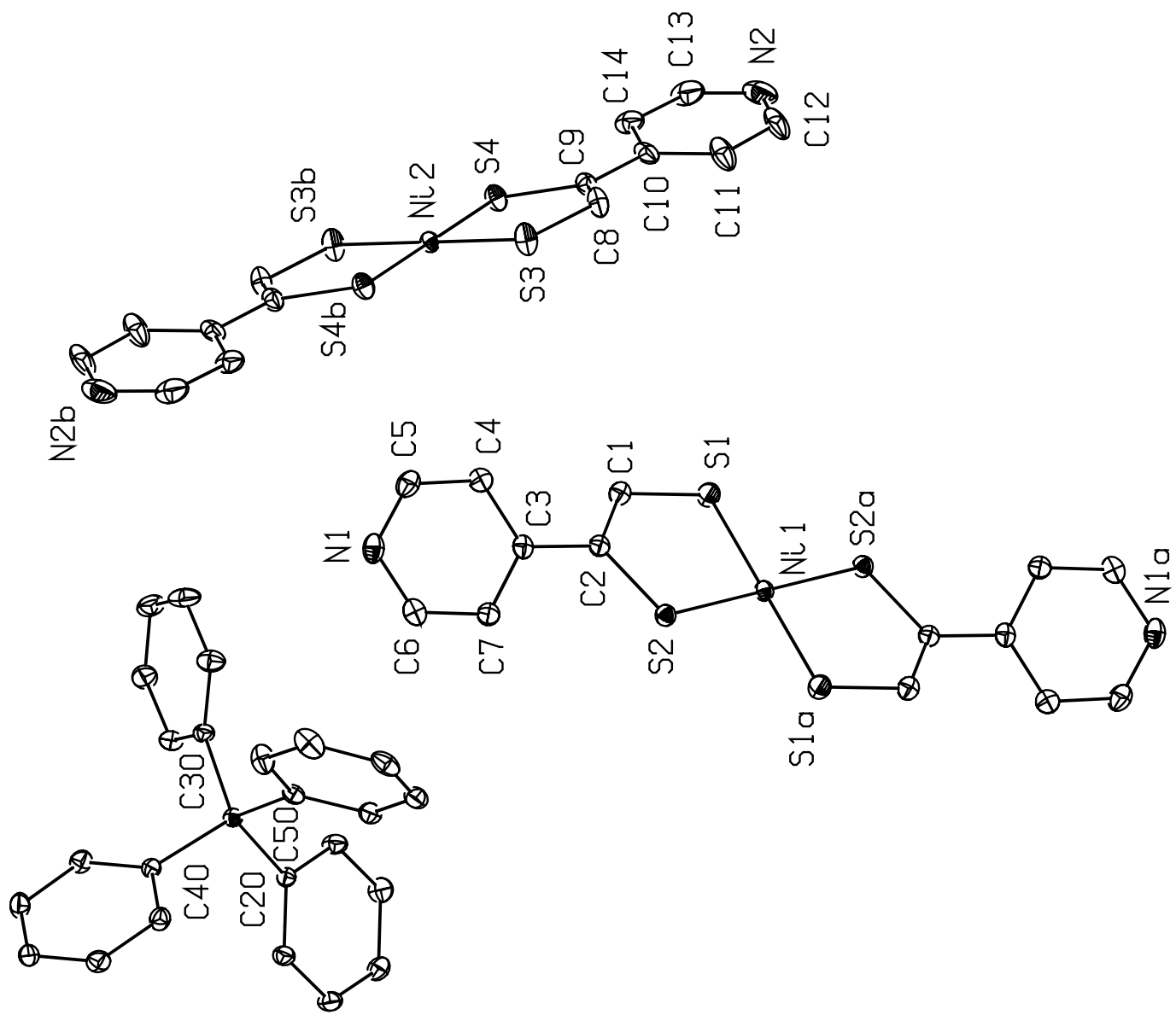


Figure 2

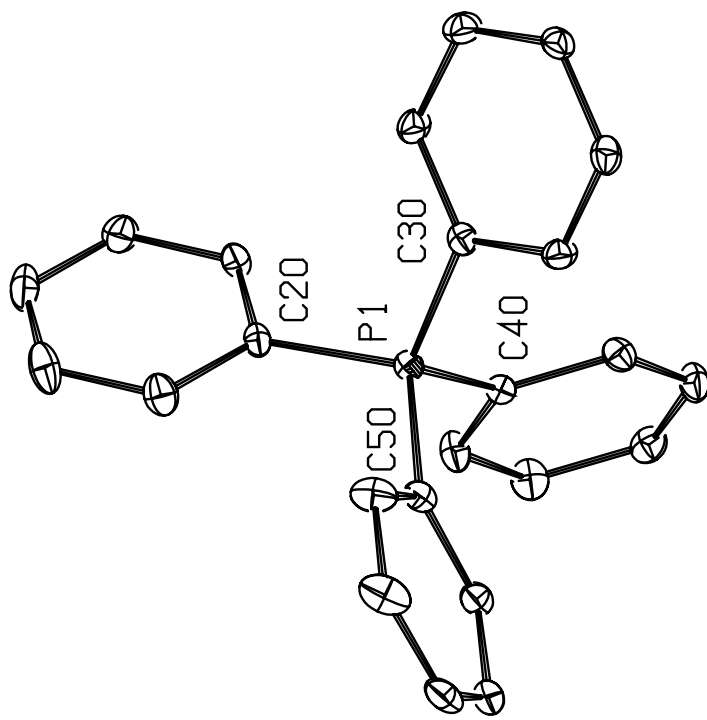
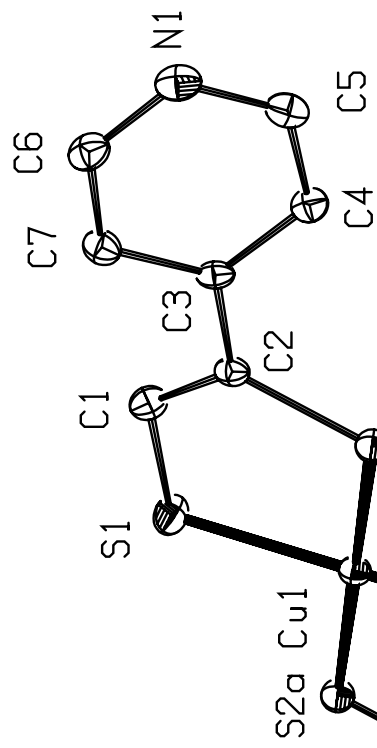
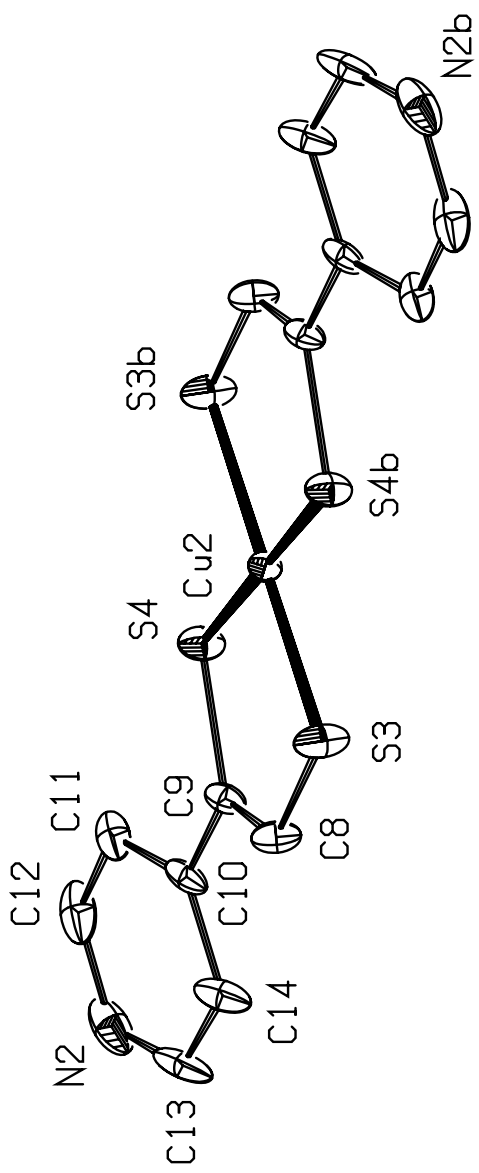


Figure3

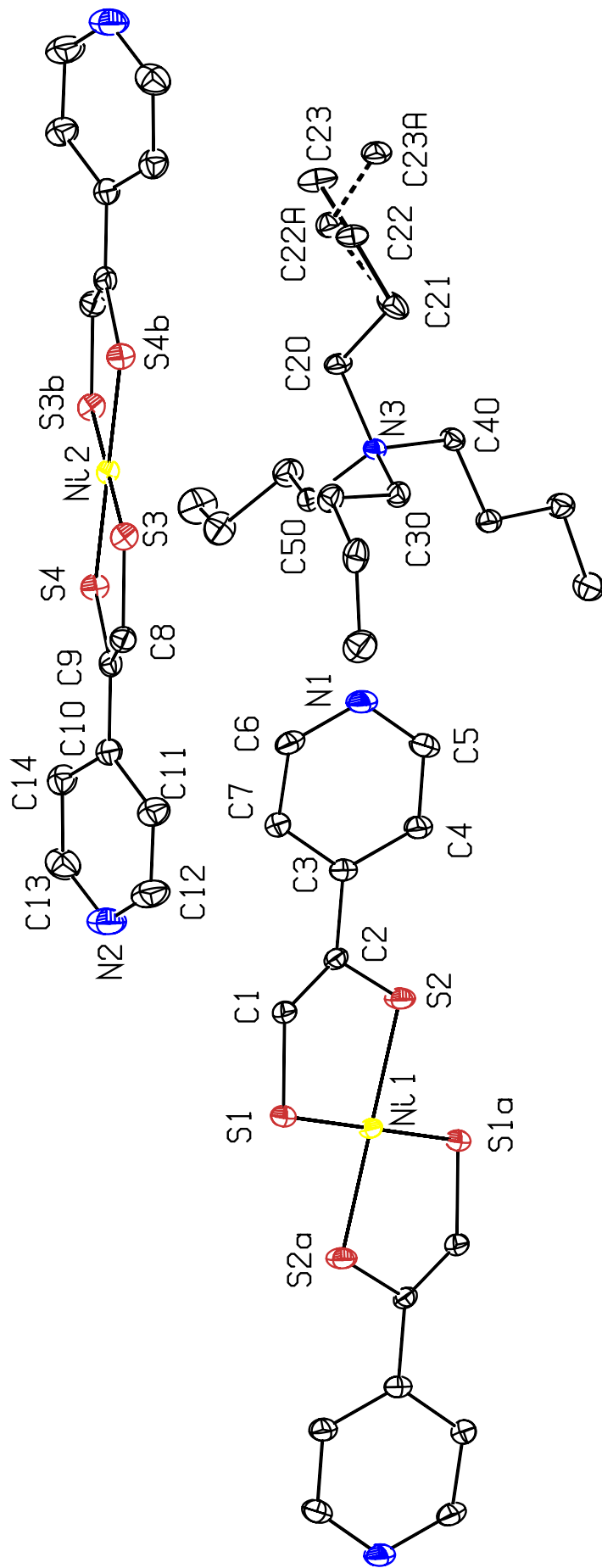


Figure 4

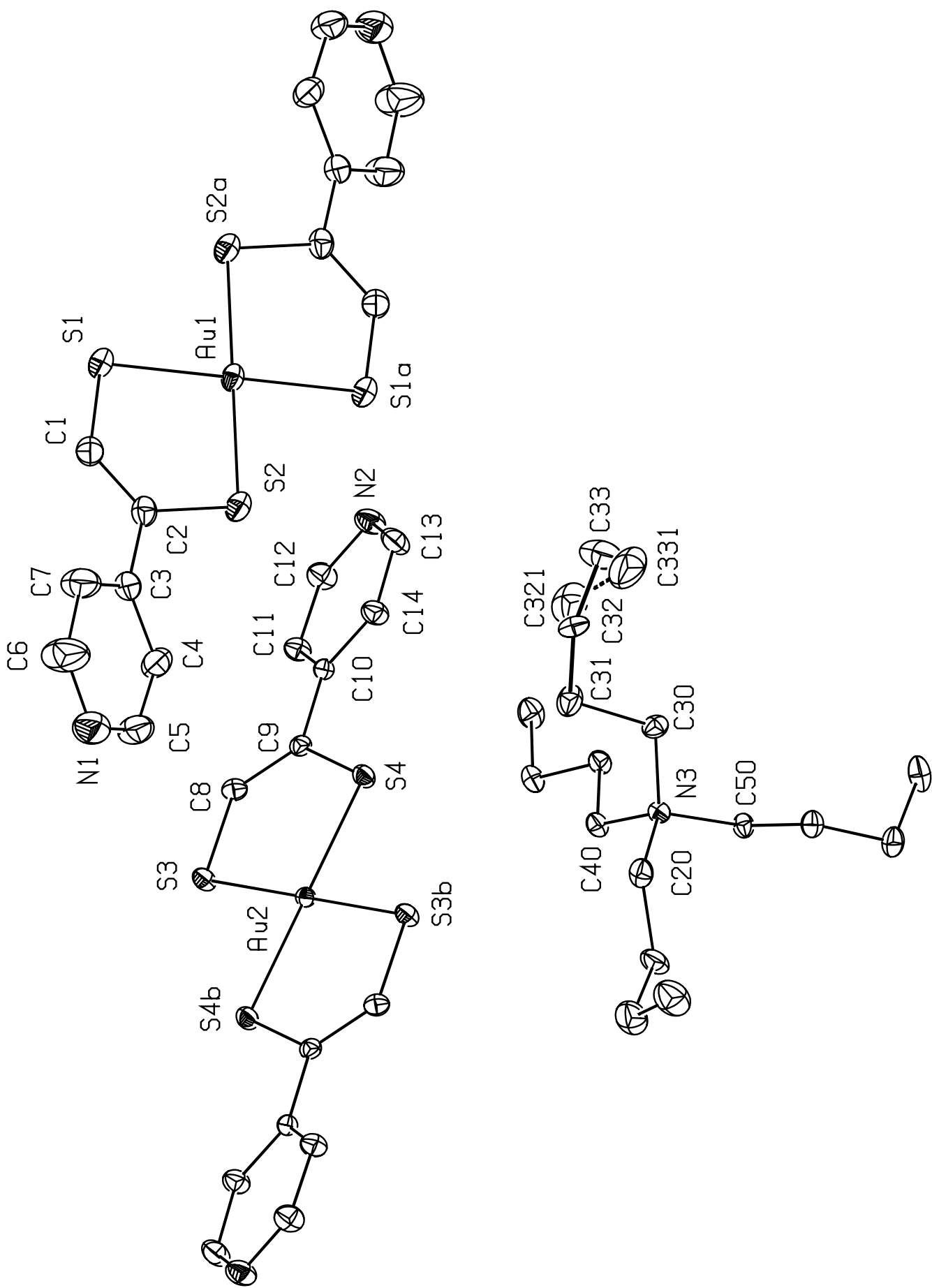


Figure 5

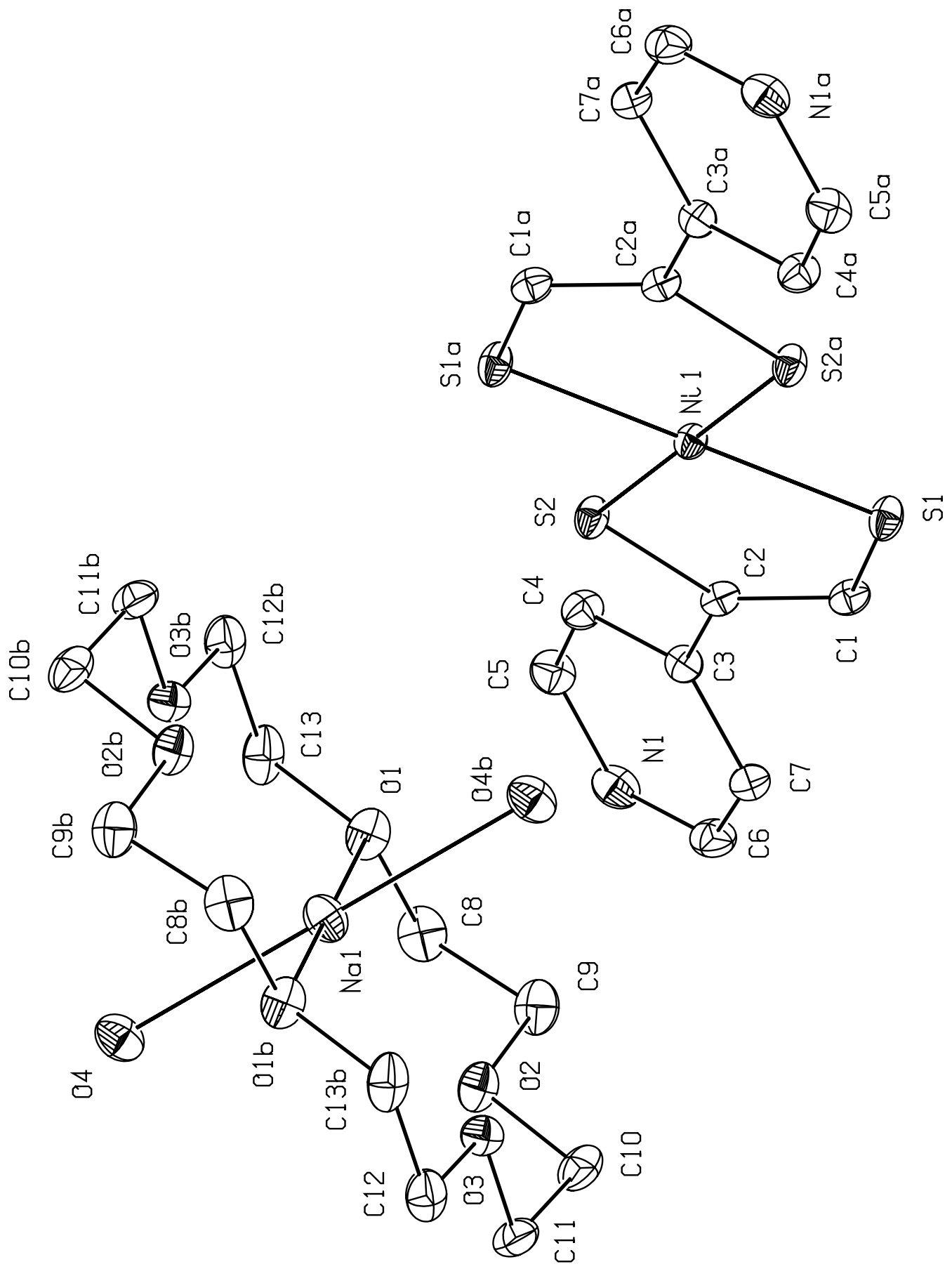


Figure6
[Click here to download high resolution image](#)

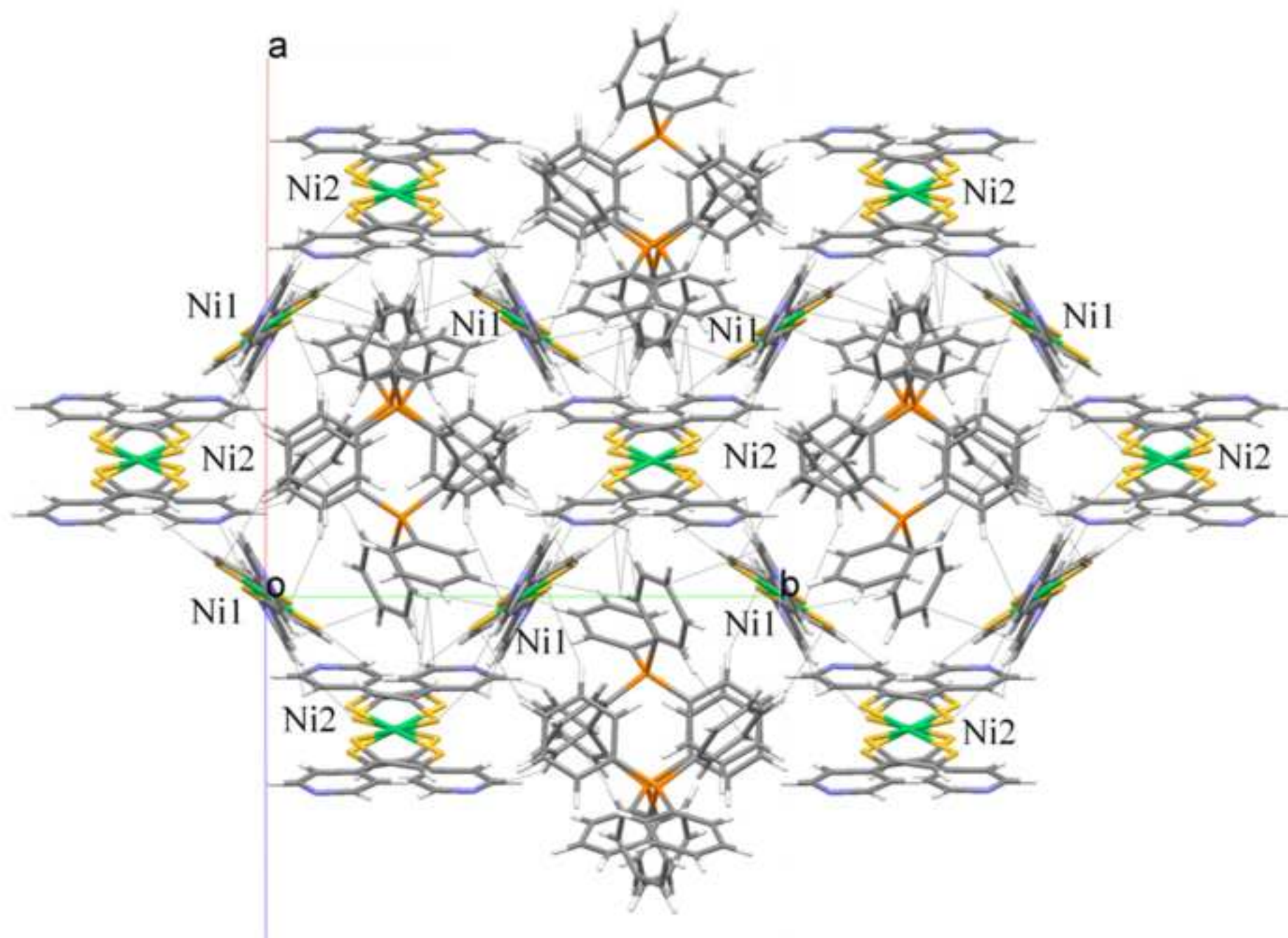


Figure7
[Click here to download high resolution image](#)

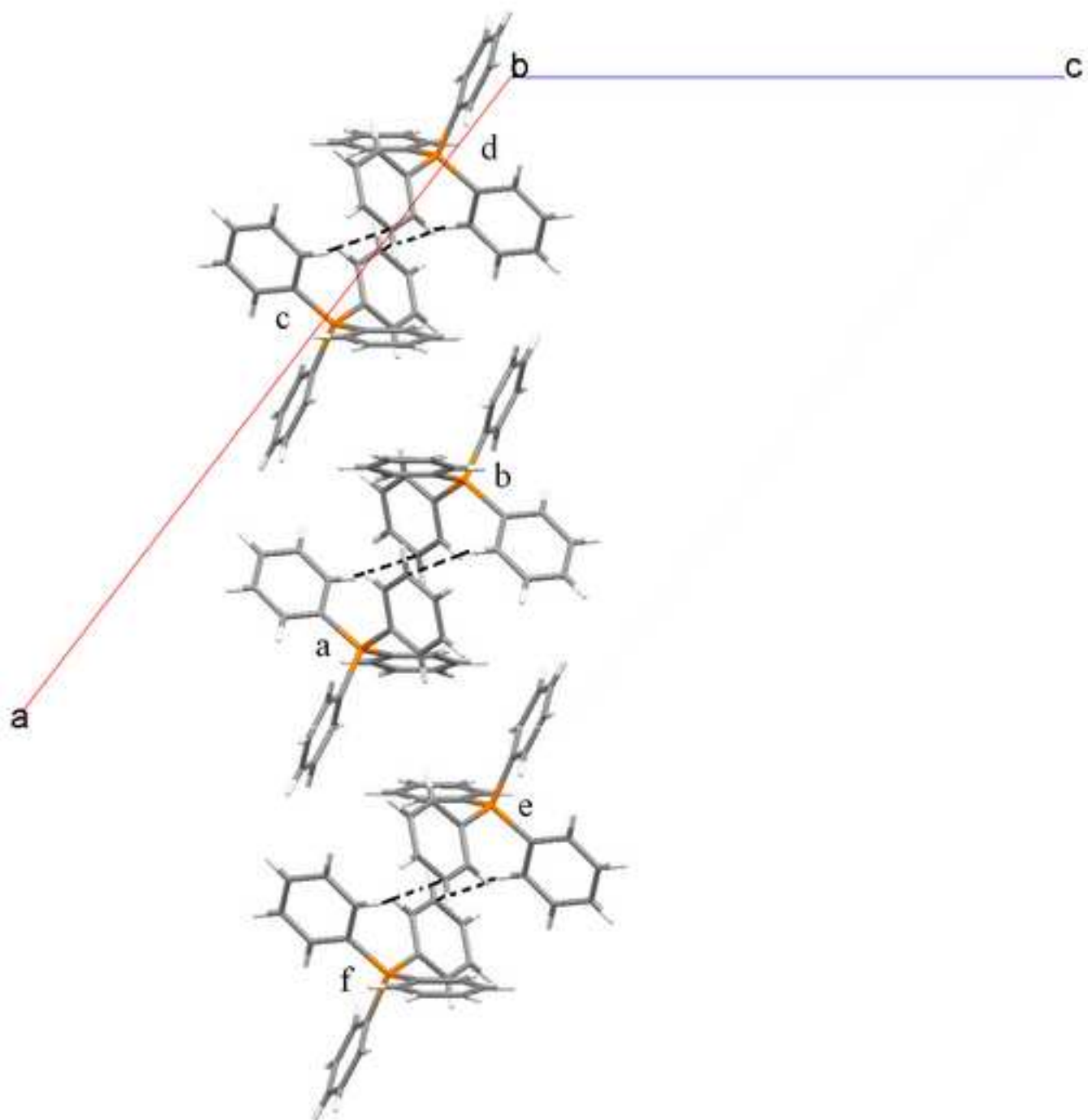


Figure8
[Click here to download high resolution image](#)

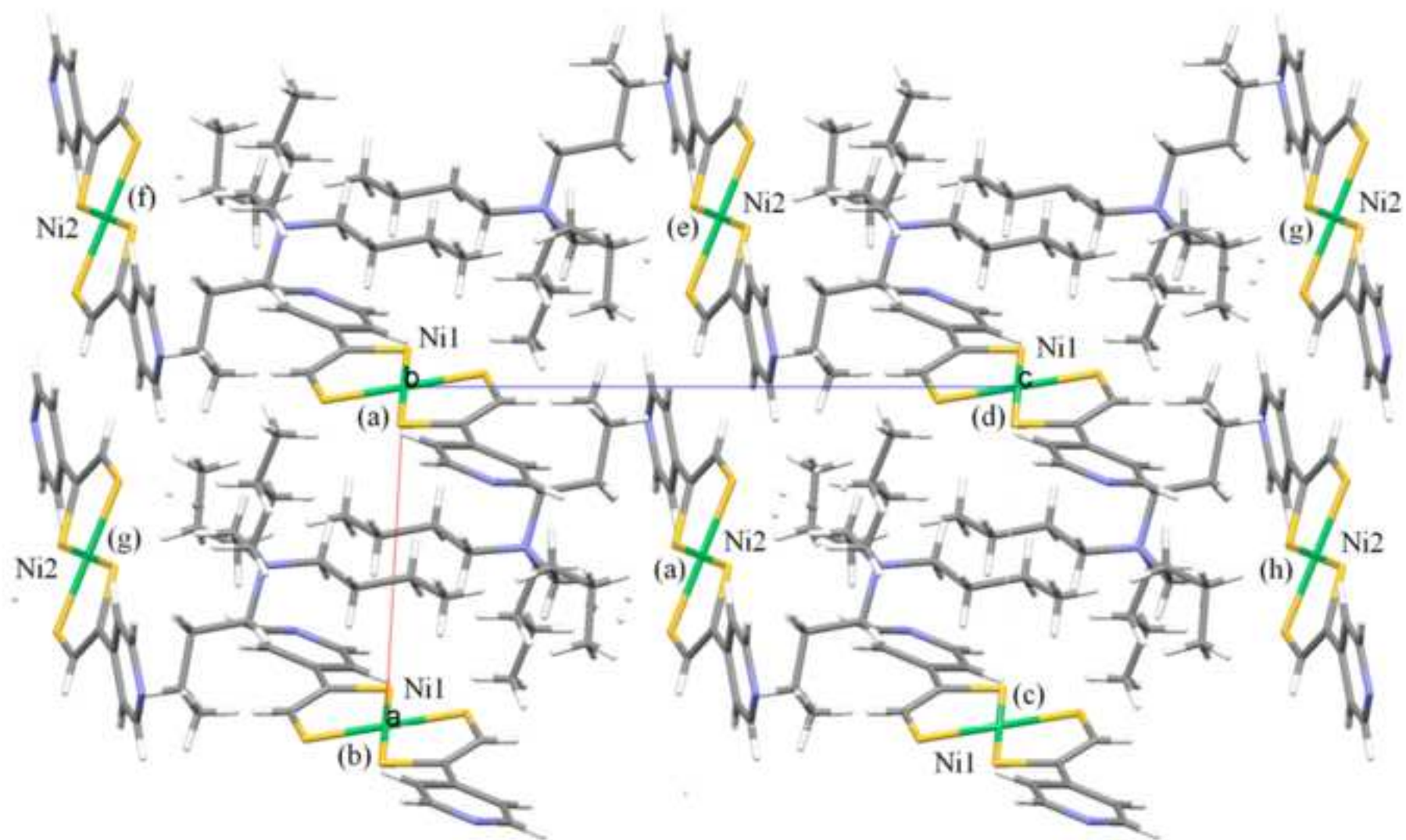


Figure9
[Click here to download high resolution image](#)

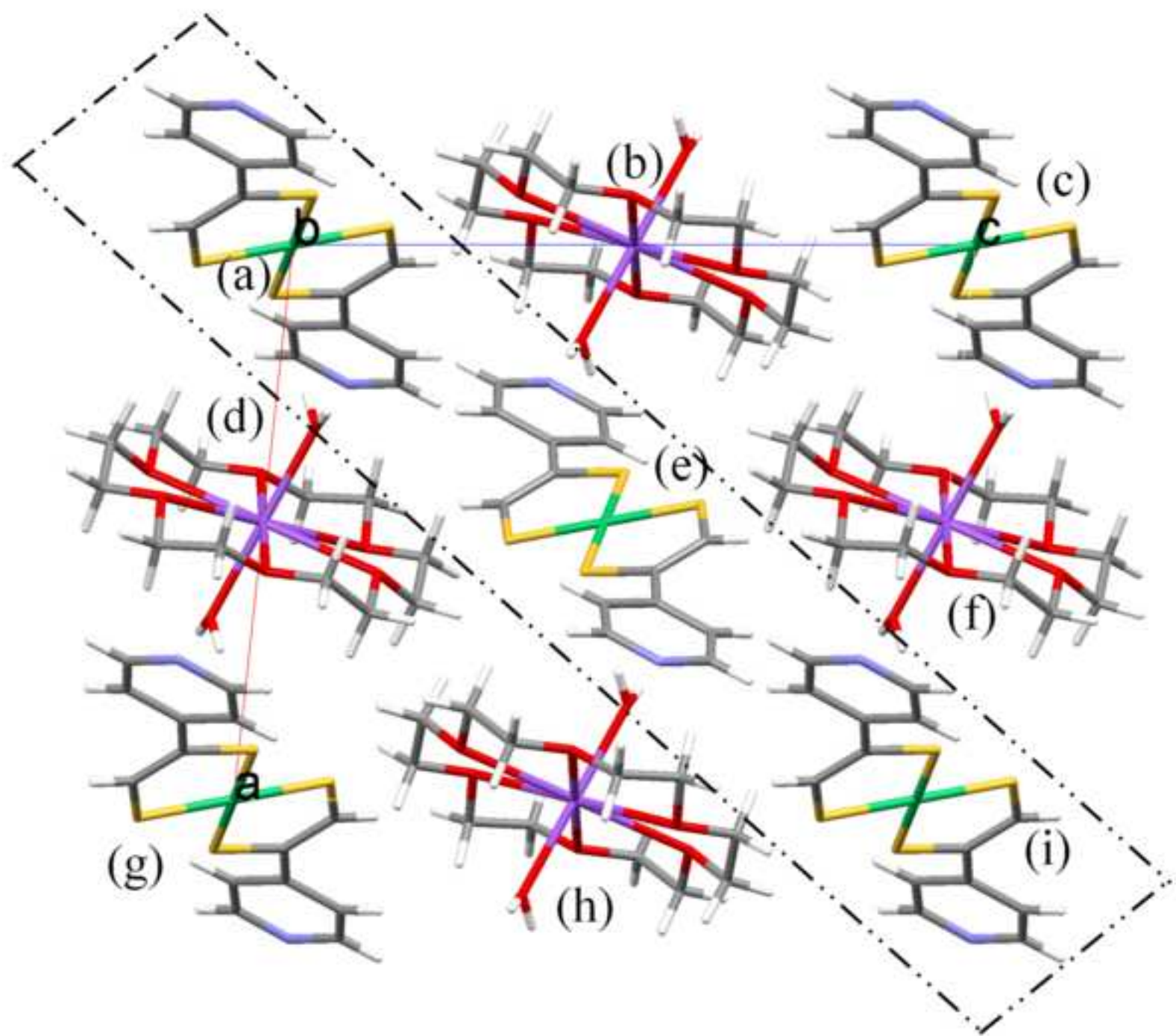
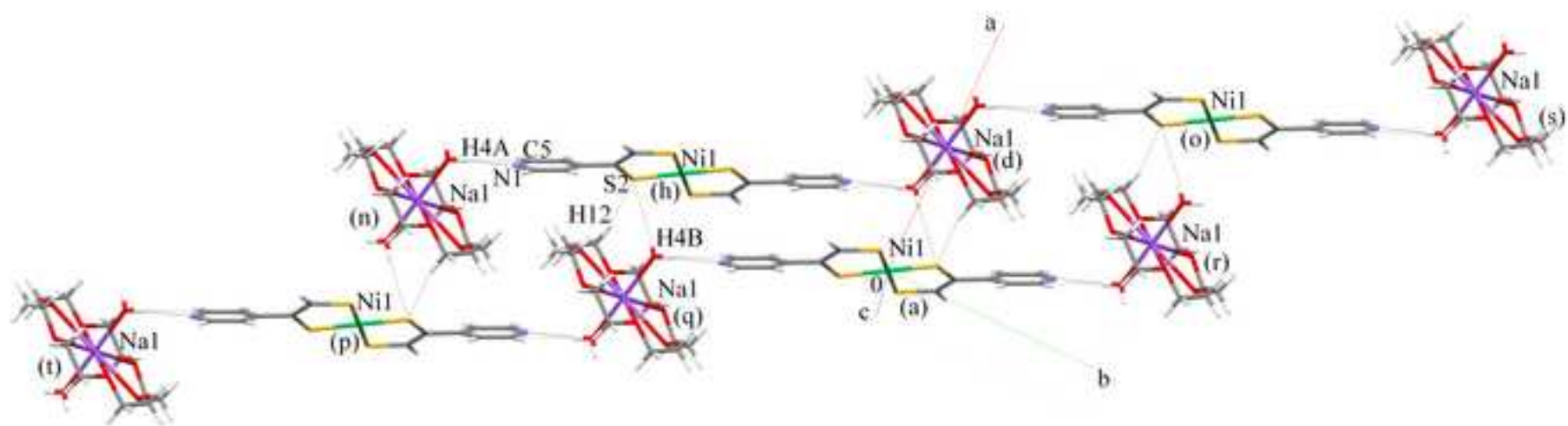
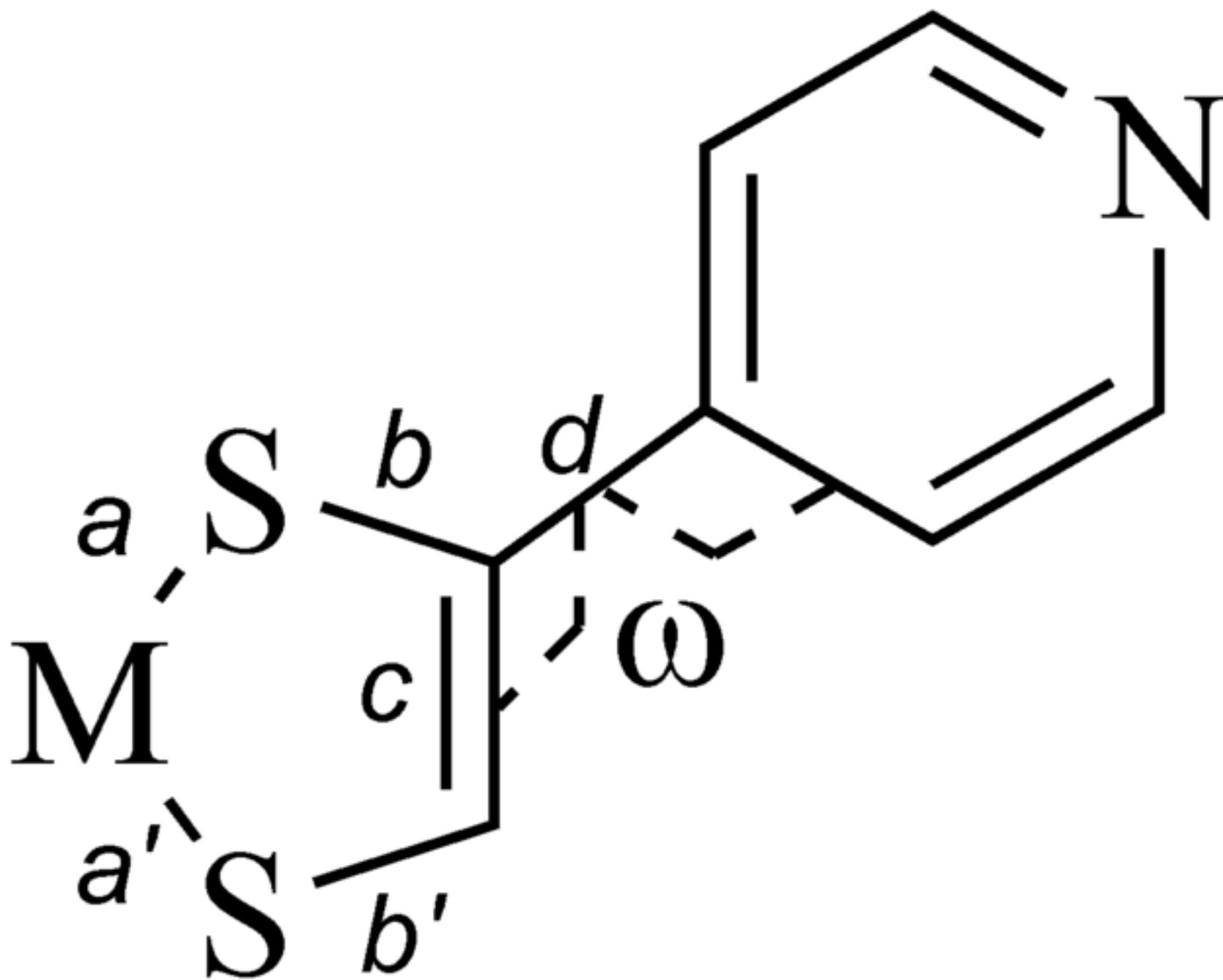


Figure10
[Click here to download high resolution image](#)

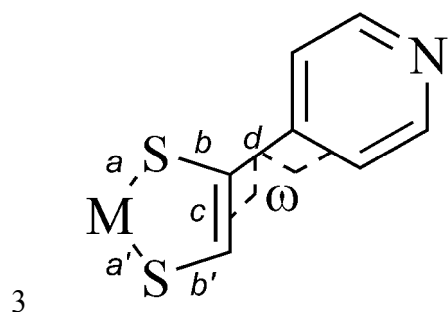


1 Table 1 - Crystallographic data and refinement parameters for complexes $\text{Ph}_4\text{P}[\text{Ni}(4\text{-pedt})_2]$ (**1**), $\text{Ph}_4\text{P}[\text{Cu}(4\text{-pedt})_2]$ (**2**), $n\text{-Bu}_4\text{N}[\text{Ni}(4\text{-pedt})_2]$ (**3**),
 2 $n\text{-Bu}_4\text{N}[\text{Au}(4\text{-pedt})_2]$ (**5**) and $[\text{Na}(18\text{c}6)][\text{Ni}(4\text{-pedt})_2]\cdot 2\text{H}_2\text{O}$ (**6·2H₂O**).

Compound	1	2	3	5	6·2H₂O
Formula	$\text{C}_{38}\text{H}_{30}\text{N}_2\text{NiP}_2\text{S}_4$	$\text{C}_{38}\text{H}_{30}\text{CuN}_2\text{P}_2\text{S}_4$	$\text{C}_{30}\text{H}_{46}\text{N}_3\text{NiS}_4$	$\text{C}_{30}\text{H}_{46}\text{AuN}_3\text{S}_4$	$\text{C}_{26}\text{H}_{38}\text{N}_2\text{NaNiO}_8\text{S}_4$
Formula weight (g mol ⁻¹)	732.58	737.39	635.65	773.90	712.49
Wavelength (Å)	0.71073	0.71073	0.71073	0.71073	0.71073
Crystal system, Space group	Monoclinic, <i>C2/c</i>	Monoclinic, <i>C2/c</i>	Triclinic, <i>P-1</i>	Triclinic, <i>P-1</i>	Monoclinic, <i>P2₁/n</i>
<i>a</i> (Å)	26.8750(5)	26.9179(8)	9.0033(2)	8.6211(1)	11.7067(14)
<i>b</i> (Å)	17.3528(3)	17.3541(6)	11.2258(2)	11.1196(2)	9.7243(12)
<i>c</i> (Å)	18.1609(3)	18.1969(5)	16.9070(3)	17.6962(3)	14.3179(18)
α (°)	90	90	107.7870(10)	74.646(1)	90
β (°)	127.5650(10)	127.3820(10)	90.3960(10)	88.829(1)	96.103(2)
γ (°)	90	90	98.3450(10)	80.336(1)	90
<i>V</i> (Å ³), <i>Z</i>	6713.4(2), 8	6754.5(4), 8	1607.48(5), 2	1612.14(4), 2	1620.7(3), 2
ρ_{calc} (Mg/m ³), μ (mm ⁻¹)	1.450, 0.906	1.450, 0.973	1.313, 0.887	1.594, 4.846	1.468, 0.918
<i>F</i> (000)	3032	3040	678	780	750
Crystal size (mm)	0.4 x 0.3 x 0.08	0.30 x 0.20 x 0.16	0.28 x 0.24 x 0.20	0.38 x 0.30 x 0.28	0.20 x 0.12 x 0.10
θ Range (°)	2.83 to 25.03	2.74 to 25.68	3.21 to 25.35	2.64 to 25.68	2.73 to 25.68
Collected <i>hkl</i>	-31 ≤ <i>h</i> ≤ 31 -20 ≤ <i>k</i> ≤ 20 -21 ≤ <i>l</i> ≤ 21	-32 ≤ <i>h</i> ≤ 32 -21 ≤ <i>k</i> ≤ 21 -20 ≤ <i>l</i> ≤ 22	-10 ≤ <i>h</i> ≤ 10 -13 ≤ <i>k</i> ≤ 13 -20 ≤ <i>l</i> ≤ 20	-10 ≤ <i>h</i> ≤ 10 -13 ≤ <i>k</i> ≤ 13 -21 ≤ <i>l</i> ≤ 21	-14 ≤ <i>h</i> ≤ 12 -11 ≤ <i>k</i> ≤ 11 -17 ≤ <i>l</i> ≤ 17
Reflections collected	41666	23618	13680	17908	7273
Independent reflections	5910 [R(int) = 0.0424]	6409 [R(int) = 0.0656]	5821 [R(int) = 0.0422]	6122 [R(int) = 0.0306]	3051 [R(int) = 0.0414]
Completeness to θ	25.03 99.7 %	25.68 99.7 %	25.35 98.9 %	25.68 99.7 %	25.68 99.3 %
Absorption correction	Semi-empirical from equivalents				
Max. and min. transmission	0.8052 and 0.7133	0.8599 and 0.7590	0.8425 and 0.7893	0.3440 and 0.2603	0.9139 and 0.8378
Refinement method	Full-matrix least-squares on <i>F</i> ²				
Data / restraints / parameters	5910 / 0 / 418	6409 / 0 / 418	5821 / 6 / 370	6122 / 2 / 370	3051 / 2 / 201
Goodness-of-fit on <i>F</i> ²	1.069	1.049	1.079	1.071	1.035
Final <i>R</i> indices [<i>I</i> > 2 σ (<i>I</i>)]	<i>R</i> ₁ = 0.0276, <i>wR</i> ₂ = 0.0711	<i>R</i> ₁ = 0.0396, <i>wR</i> ₂ = 0.0868	<i>R</i> ₁ = 0.0366, <i>wR</i> ₂ = 0.0899	<i>R</i> ₁ = 0.0254, <i>wR</i> ₂ = 0.0590	<i>R</i> ₁ = 0.0376, <i>wR</i> ₂ = 0.0791
<i>R</i> indices (all data)	<i>R</i> ₁ = 0.0341, <i>wR</i> ₂ = 0.0740	<i>R</i> ₁ = 0.0644, <i>wR</i> ₂ = 0.0945	<i>R</i> ₁ = 0.0482, <i>wR</i> ₂ = 0.0947	<i>R</i> ₁ = 0.0401, <i>wR</i> ₂ = 0.0630	<i>R</i> ₁ = 0.0659, <i>wR</i> ₂ = 0.0853
Larg. diff. peak and hole (e Å ⁻³)	0.416 and -0.355	0.422 and -0.473	0.556 and -0.280	2.348 and -0.895	0.392 and -0.502



- 1 Table 2 - Important bond lengths (in Å) within the metallocycle, the torsion angle ω (in °) between the pyridine group plane and the metallocycle
- 2 plane and δ -parameter (defined below) for compounds **1**, **2**, **3**, **5** and **6·2H₂O**.



Compound	1	3	6·2H₂O	2	5				
	M = Ni2	M = Ni1	M = Ni1	M = Ni2	M = Ni	M = Cu1	M = Cu2	M = Au2	M = Au1
M-S (<i>a</i>)	2.1293(5)	2.1507(5)	2.1383(5)	2.1549(6)	2.1375(7)	2.1871(7)	2.1626(7)	2.3078(10)	2.3183(13)
M-S (<i>a'</i>)	2.1474(5)	2.1416(5)	2.1463(6)	2.1478(7)	2.1531(7)	2.1797(8)	2.1812(8)	2.3053(11)	2.3082(11)
S-C (<i>b</i>)	1.737(2)	1.742(2)	1.739(2)	1.740(3)	1.738(3)	1.771(3)	1.765(3)	1.768(4)	1.771(4)
S-C (<i>b'</i>)	1.715(2)	1.715(2)	1.713(2)	1.715(2)	1.714(3)	1.735(3)	1.740(3)	1.742(4)	1.735(5)
C=C (<i>c</i>)	1.353(3)	1.351(3)	1.364(3)	1.351(3)	1.354(4)	1.335(4)	1.328(4)	1.345(6)	1.336(6)
C-C (<i>d</i>)	1.478(3)	1.476(3)	1.474(3)	1.476(3)	1.469(4)	1.481(4)	1.483(4)	1.477(5)	1.476(7)
ω	13.14(6)	28.50(8)	29.51(8)	28.64(7)	33.56(7)	28.92(12)	13.90(8)	21.83(13)	33.44(17)
δ	1.26	1.55	1.49	1.44	1.38	2.03	1.42	1.47	2.03

4 $\delta = 100(b-b')/b$

5

1

2 Table 3. Redox potentials (mV, vs. $[\text{Fc}]^+ / [\text{Fc}]$) of **1-6** at room temperature in CH_2Cl_2
 3 containing $[\text{n-Bu}_4\text{N}] \text{PF}_6$ (0.1 M) with a 100 mVs^{-1} scan rate.

Compound	$[\text{ML}_2]^{2-} / [\text{ML}_2]^-$	$[\text{ML}_2]^- / [\text{ML}_2]^0$
$[\text{n-Ph}_4\text{P}][\text{Ni}(4\text{-pedt})_2]$ (1)	-519	297
$[\text{n-Ph}_4\text{P}][\text{Cu}(4\text{-pedt})_2]$ (2)	-374	676
$[\text{n-Bu}_4\text{N}][\text{Ni}(4\text{-pedt})_2]$ (3)	-523	303
$[\text{n-Bu}_4\text{N}][\text{Cu}(4\text{-pedt})_2]$ (4)	-379	771
$[\text{n-Bu}_4\text{N}][\text{Au}(4\text{-pedt})_2]$ (5)		585
$[\text{Na}(18\text{c}6)][\text{Ni}(4\text{-pedt})_2]$ (6)	-518	298
$[\text{Na}(18\text{c}6)][\text{Au}(4\text{-pedt})_2]$ (7)		588

4

5

CIF File (Required if manuscript contains crystal structure(s))

[Click here to download CIF File \(Required if manuscript contains crystal structure\(s\)\): Cif_1.cif](#)

CIF File (Required if manuscript contains crystal structure(s))

[Click here to download CIF File \(Required if manuscript contains crystal structure\(s\)\): Cif_2.cif](#)

CIF File (Required if manuscript contains crystal structure(s))

[Click here to download CIF File \(Required if manuscript contains crystal structure\(s\)\): Cif_3.cif](#)

CIF File (Required if manuscript contains crystal structure(s))

[Click here to download CIF File \(Required if manuscript contains crystal structure\(s\)\): Cif_4.cif](#)

CIF File (Required if manuscript contains crystal structure(s))

[Click here to download CIF File \(Required if manuscript contains crystal structure\(s\)\): Cif_5.cif](#)

CIF File (Required if manuscript contains crystal structure(s))

[Click here to download CIF File \(Required if manuscript contains crystal structure\(s\)\): Cif_6_2H2O.cif](#)

CIF Validation Report (Recommended if manuscript contains crystal structure(s))

[Click here to download CIF Validation Report \(Recommended if manuscript contains crystal structure\(s\)\): checkcif_1.pdf](#)

CIF Validation Report (Recommended if manuscript contains crystal structure(s))

[Click here to download CIF Validation Report \(Recommended if manuscript contains crystal structure\(s\)\): checkcif_2.pdf](#)

CIF Validation Report (Recommended if manuscript contains crystal structure(s))

[Click here to download CIF Validation Report \(Recommended if manuscript contains crystal structure\(s\)\): checkcif_3.pdf](#)

CIF Validation Report (Recommended if manuscript contains crystal structure(s))

[Click here to download CIF Validation Report \(Recommended if manuscript contains crystal structure\(s\)\): Checkcif_4.pdf](#)

CIF Validation Report (Recommended if manuscript contains crystal structure(s))

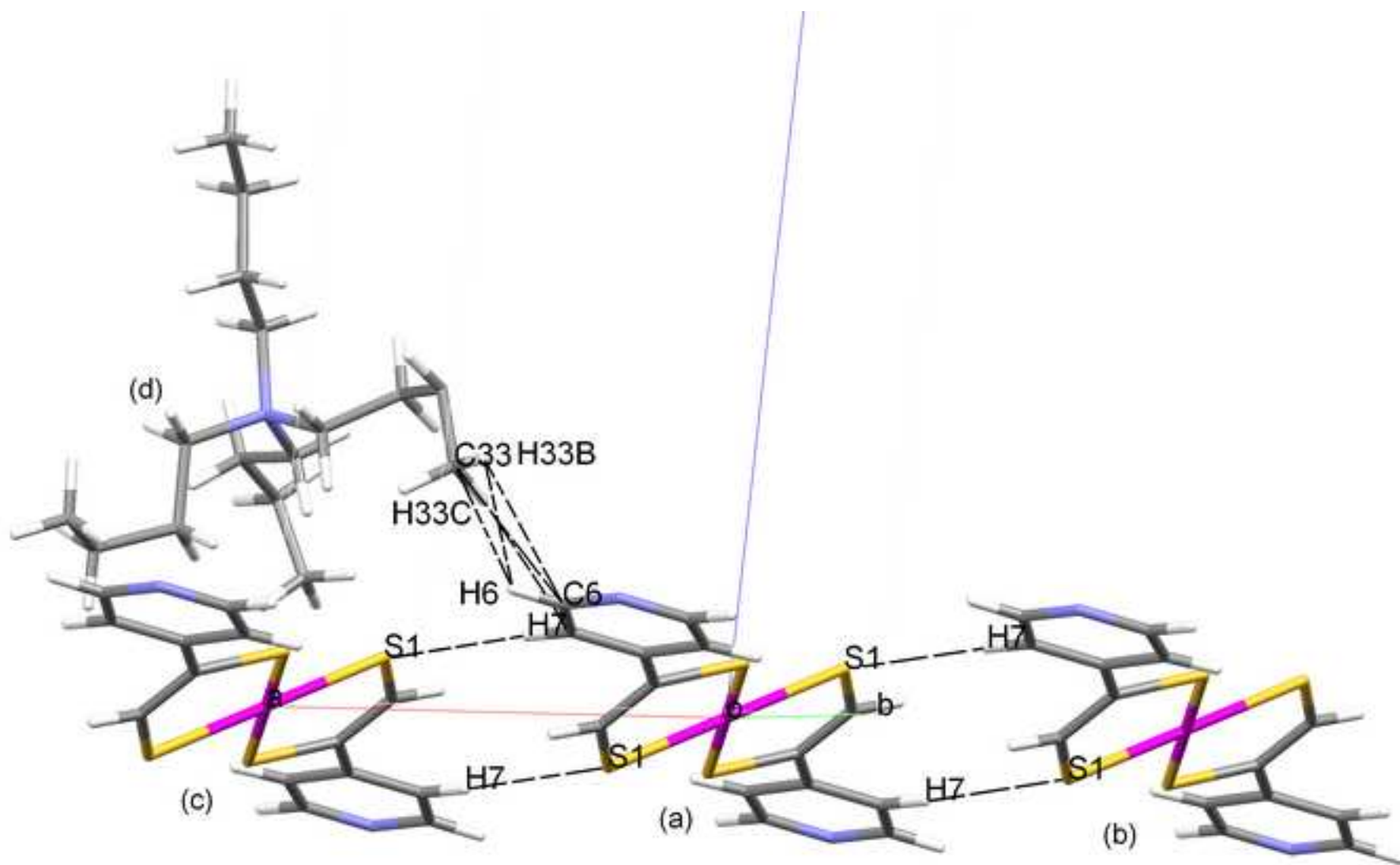
[Click here to download CIF Validation Report \(Recommended if manuscript contains crystal structure\(s\)\): checkcif_5.pdf](#)

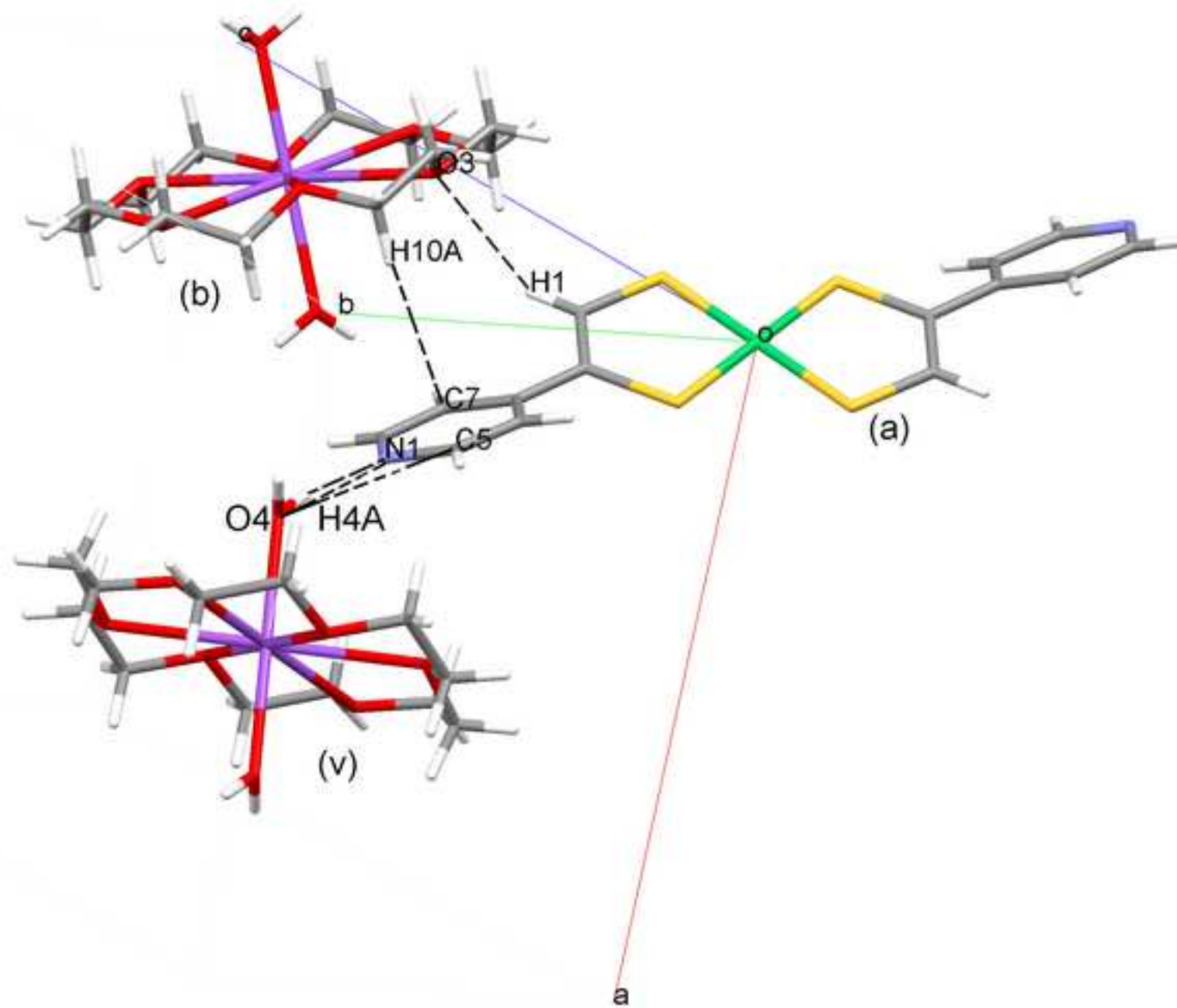
CIF Validation Report (Recommended if manuscript contains crystal structure(s))

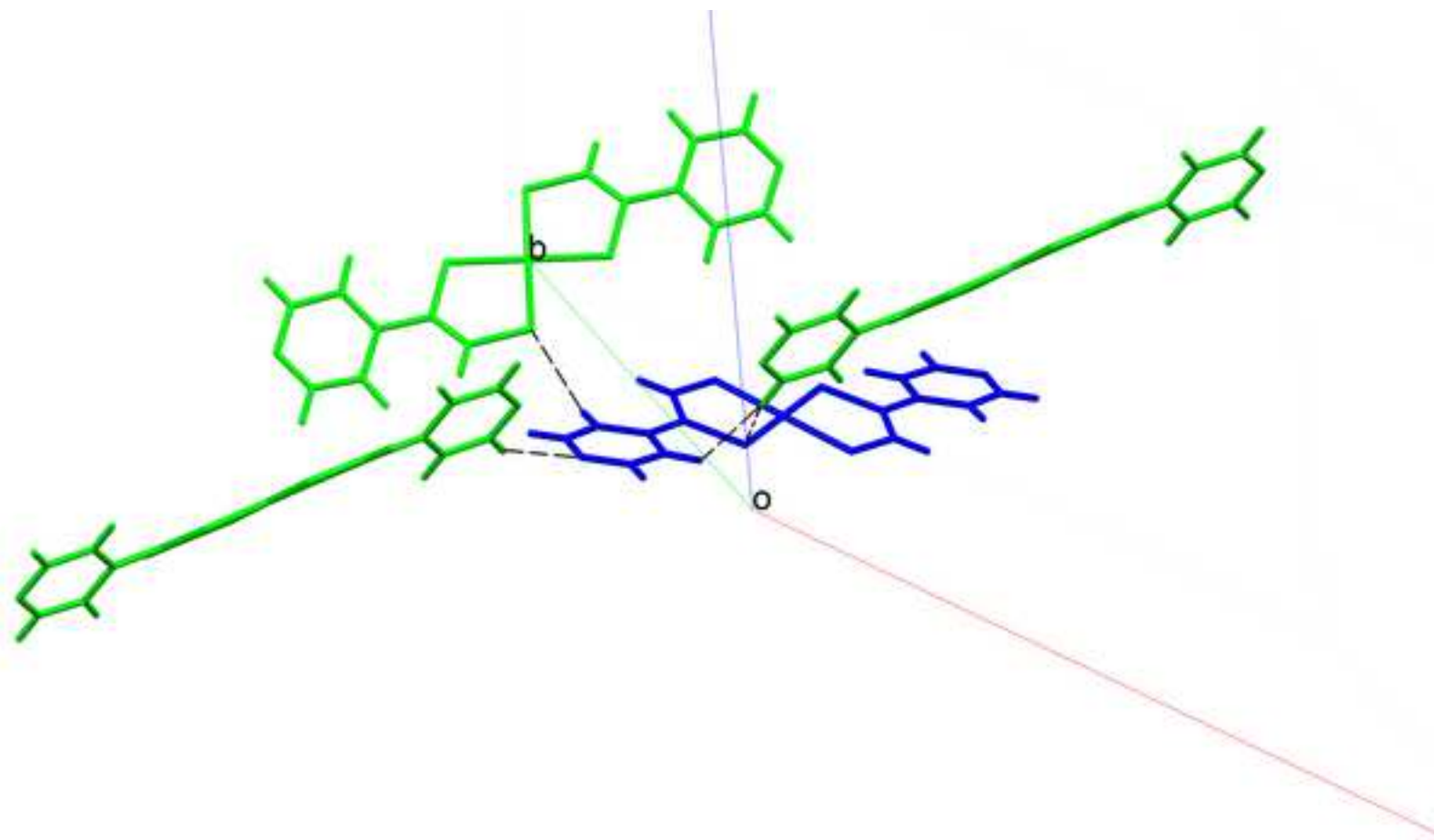
[Click here to download CIF Validation Report \(Recommended if manuscript contains crystal structure\(s\)\): checkcif_6_2H2O.pdf](#)

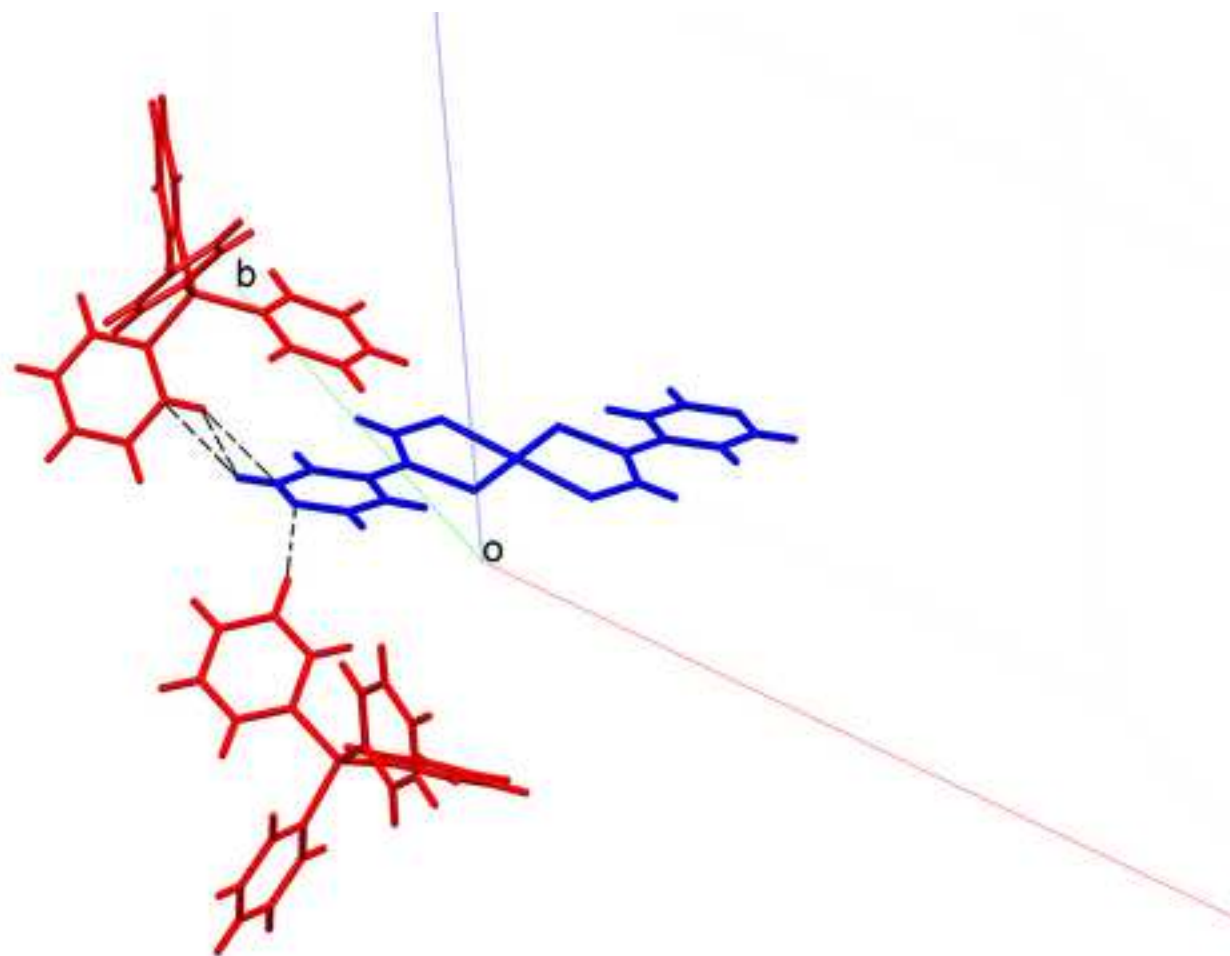
Supplementary Info for Online Publication

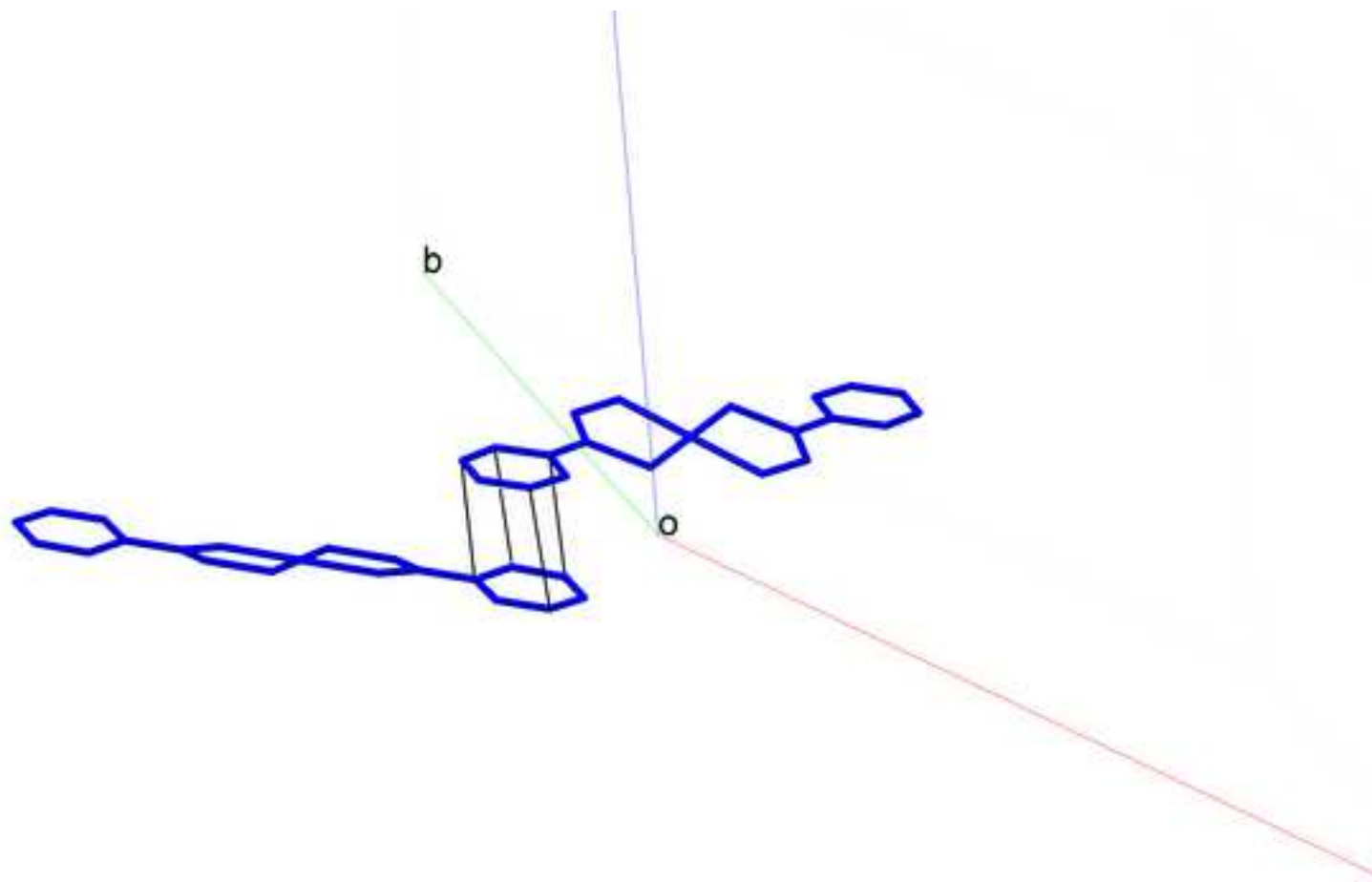
[Click here to download Supplementary Info for Online Publication: Supplementary_Info_publication_online_Revised.doc](#)

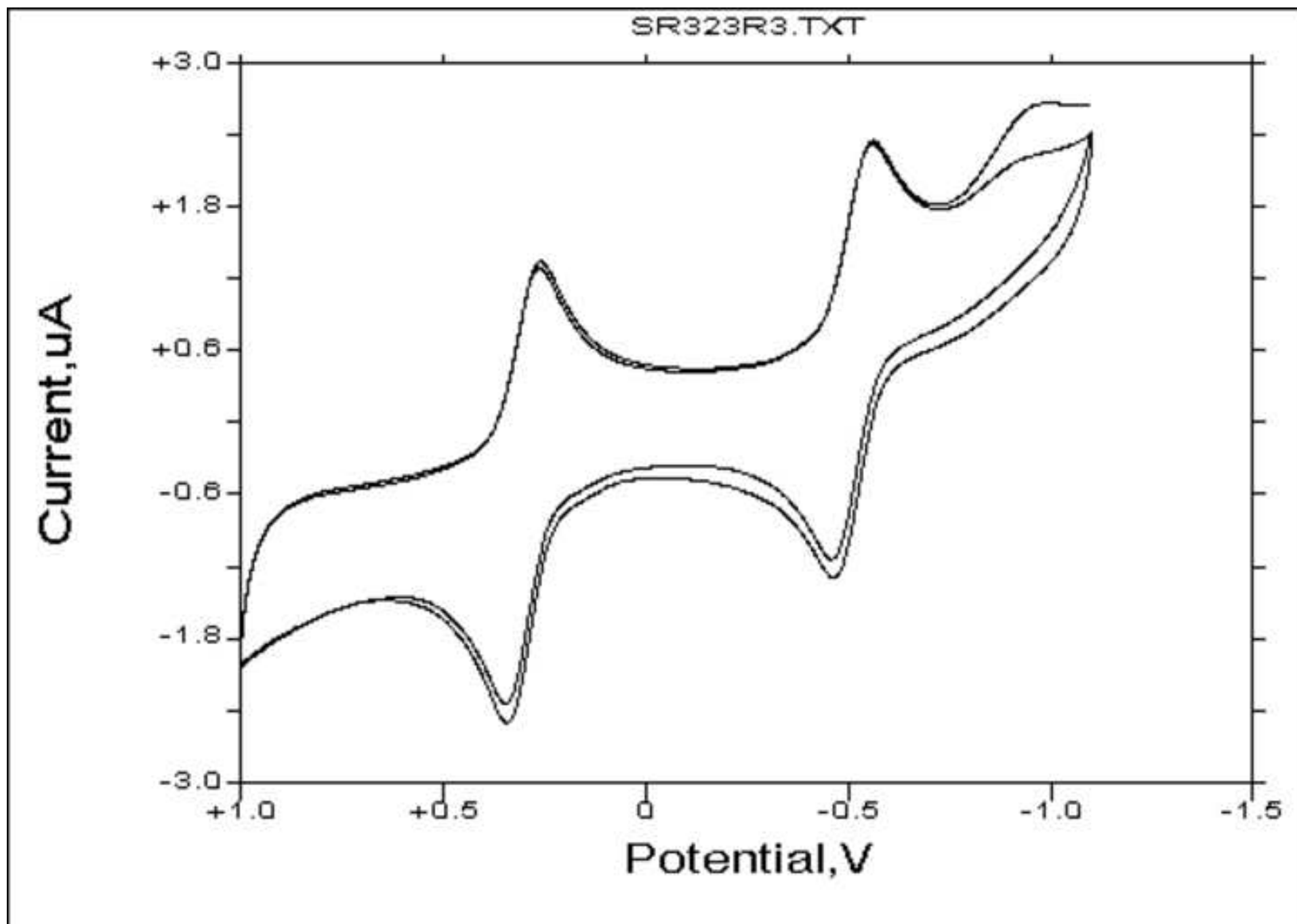


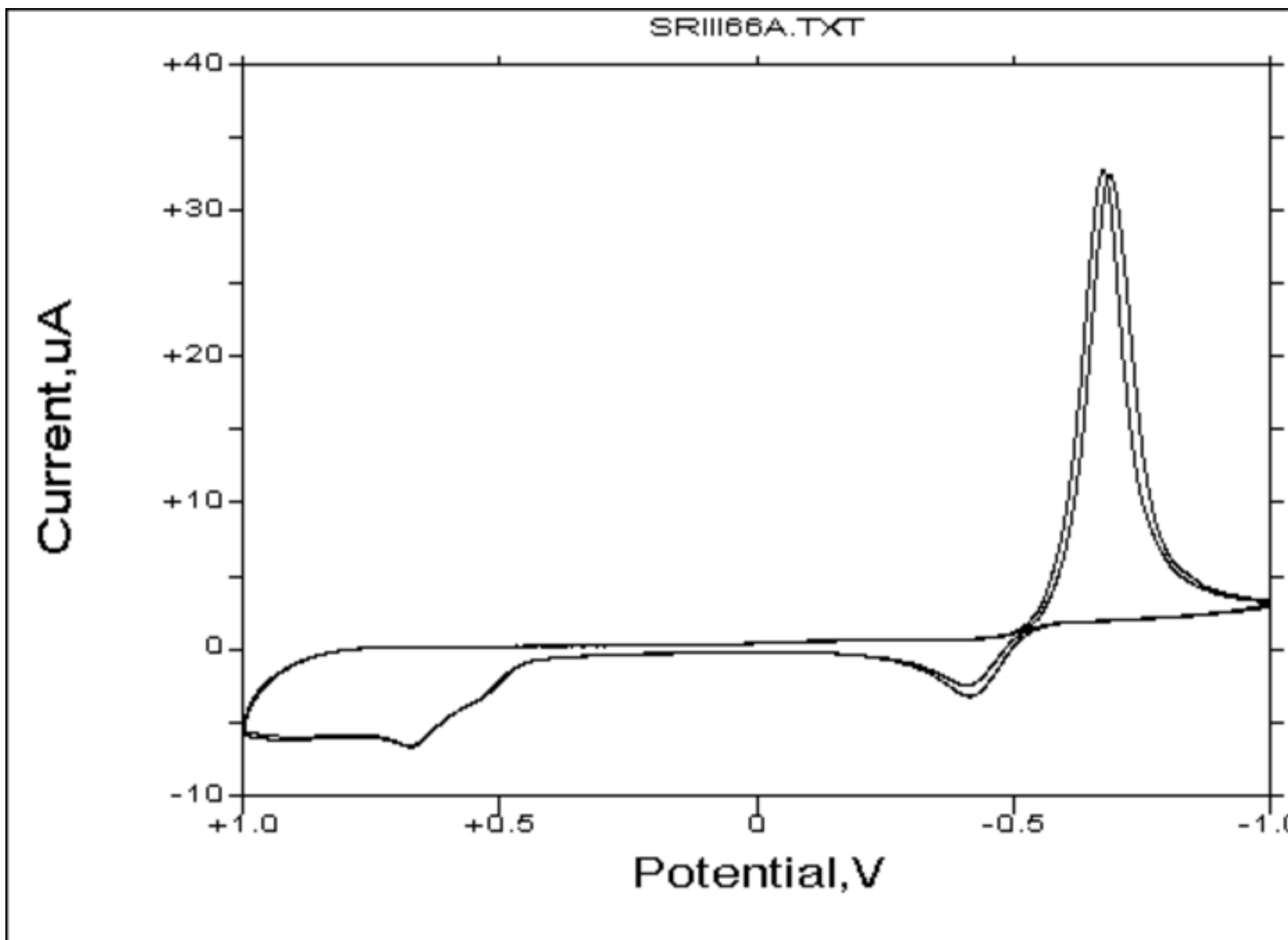


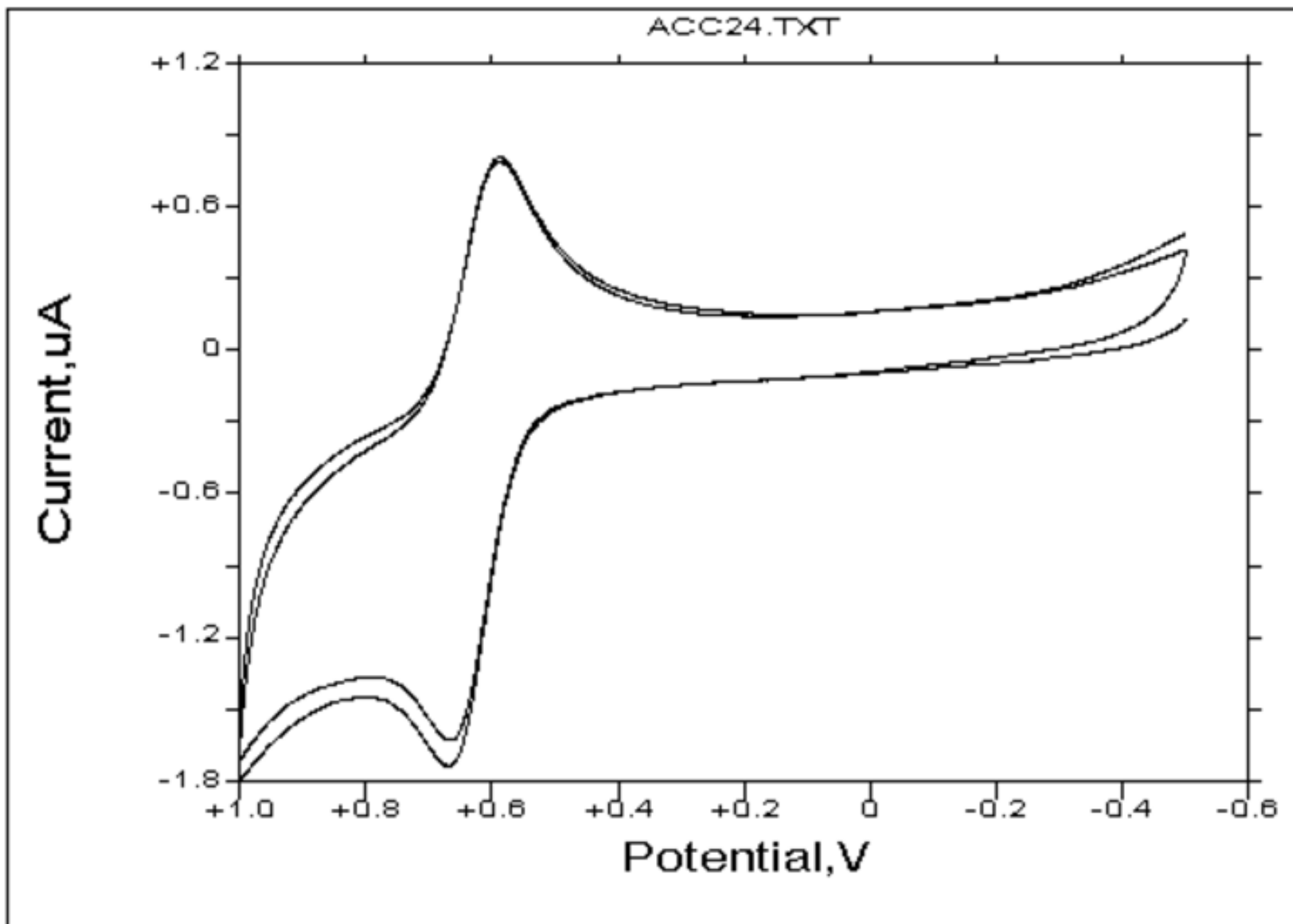


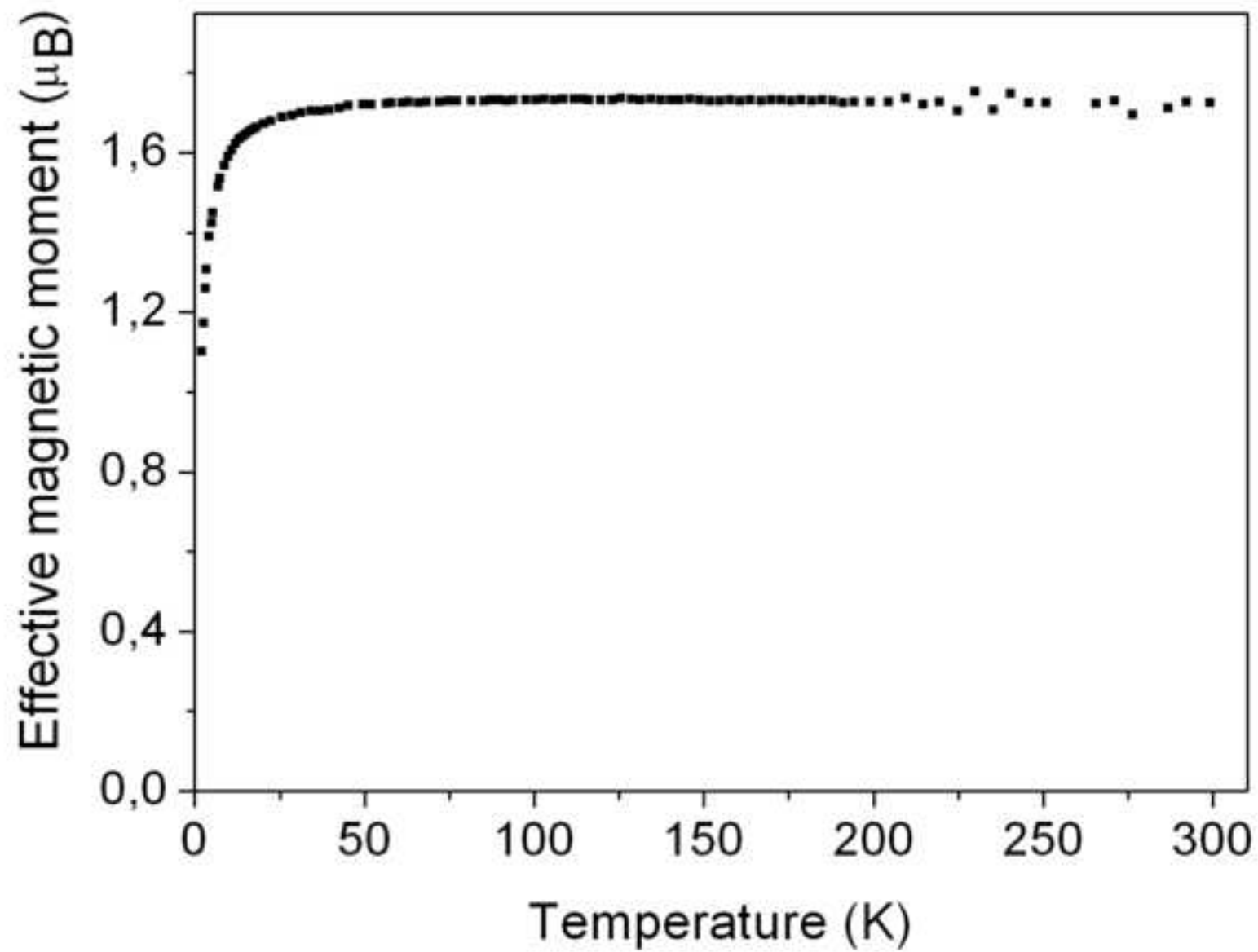


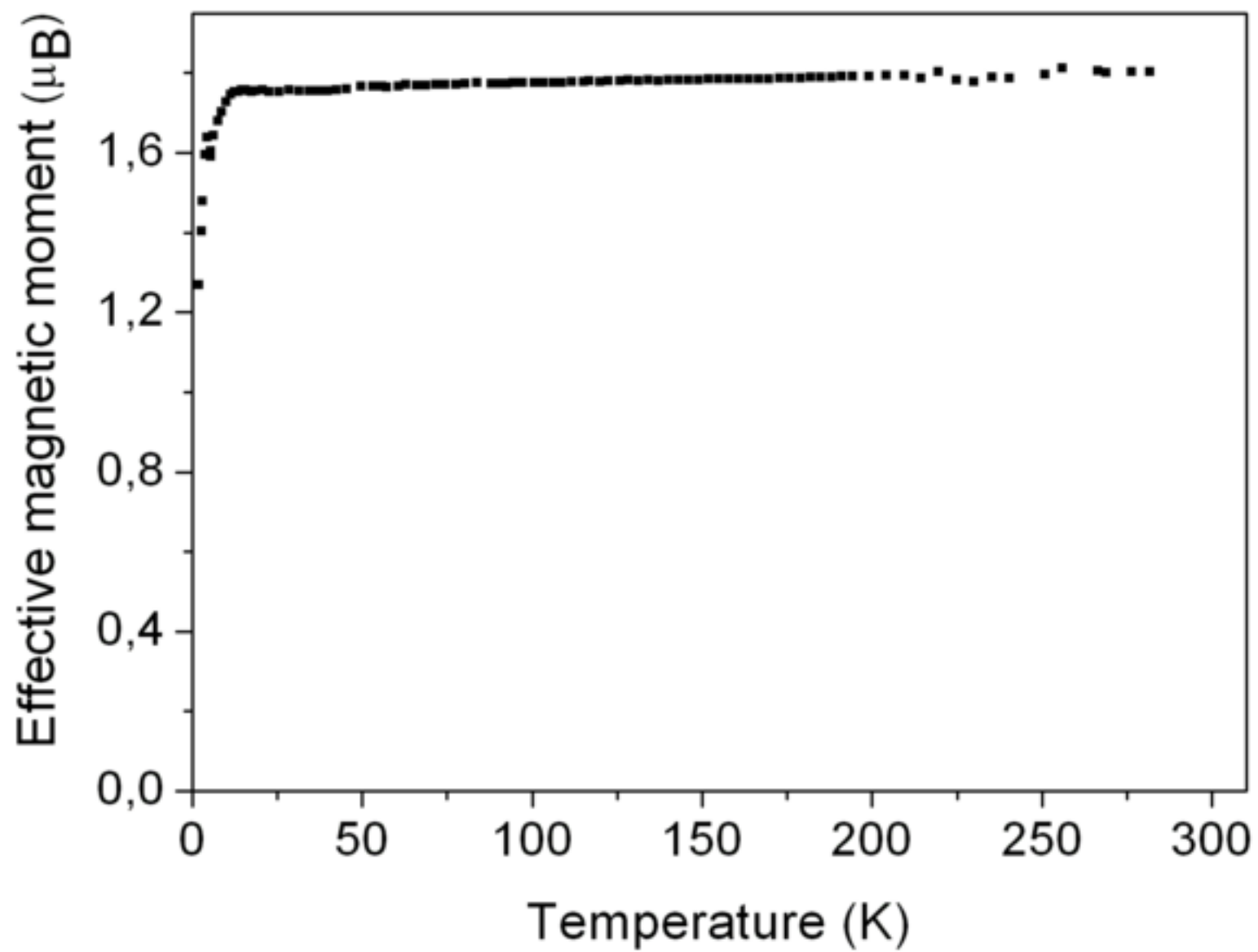


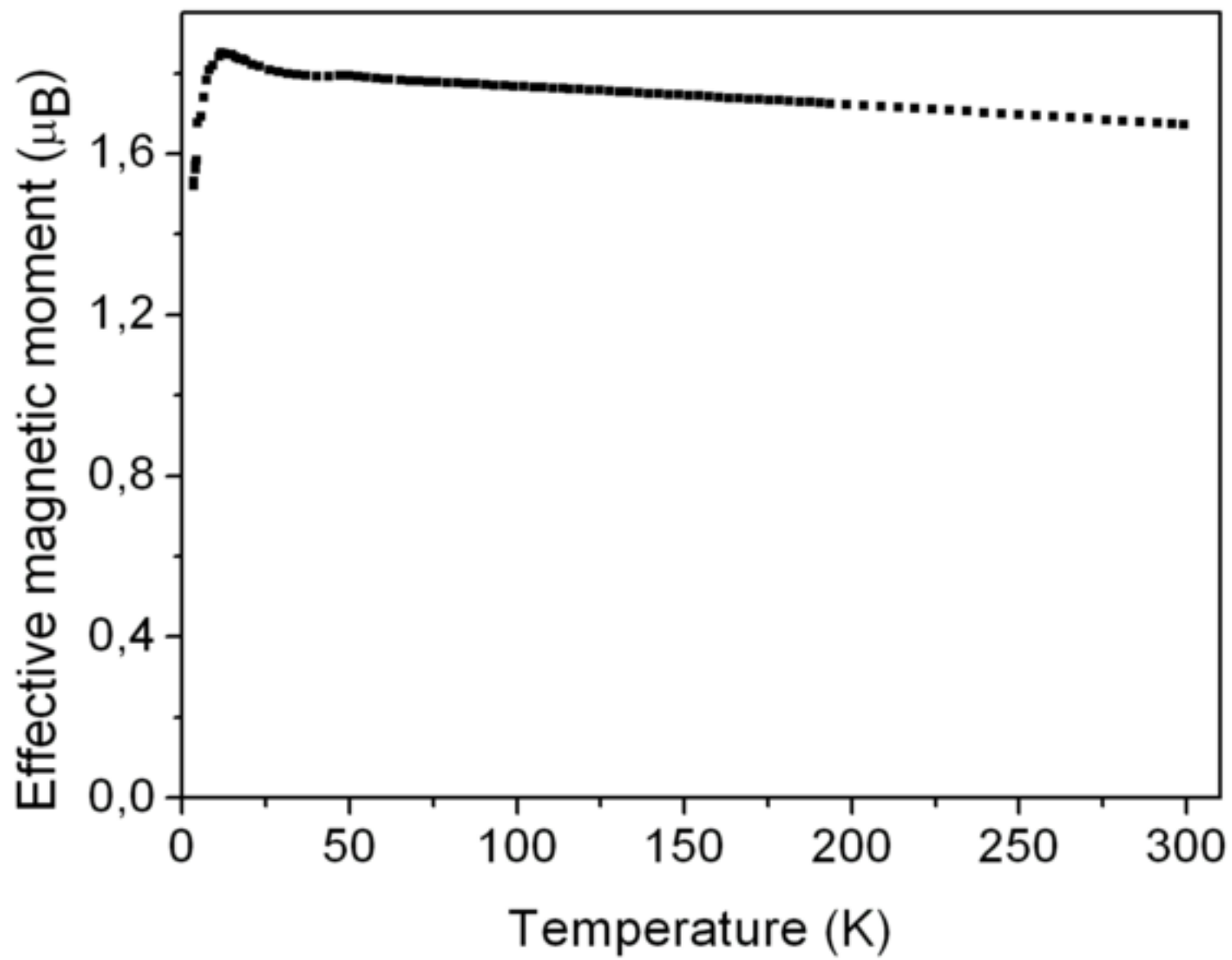


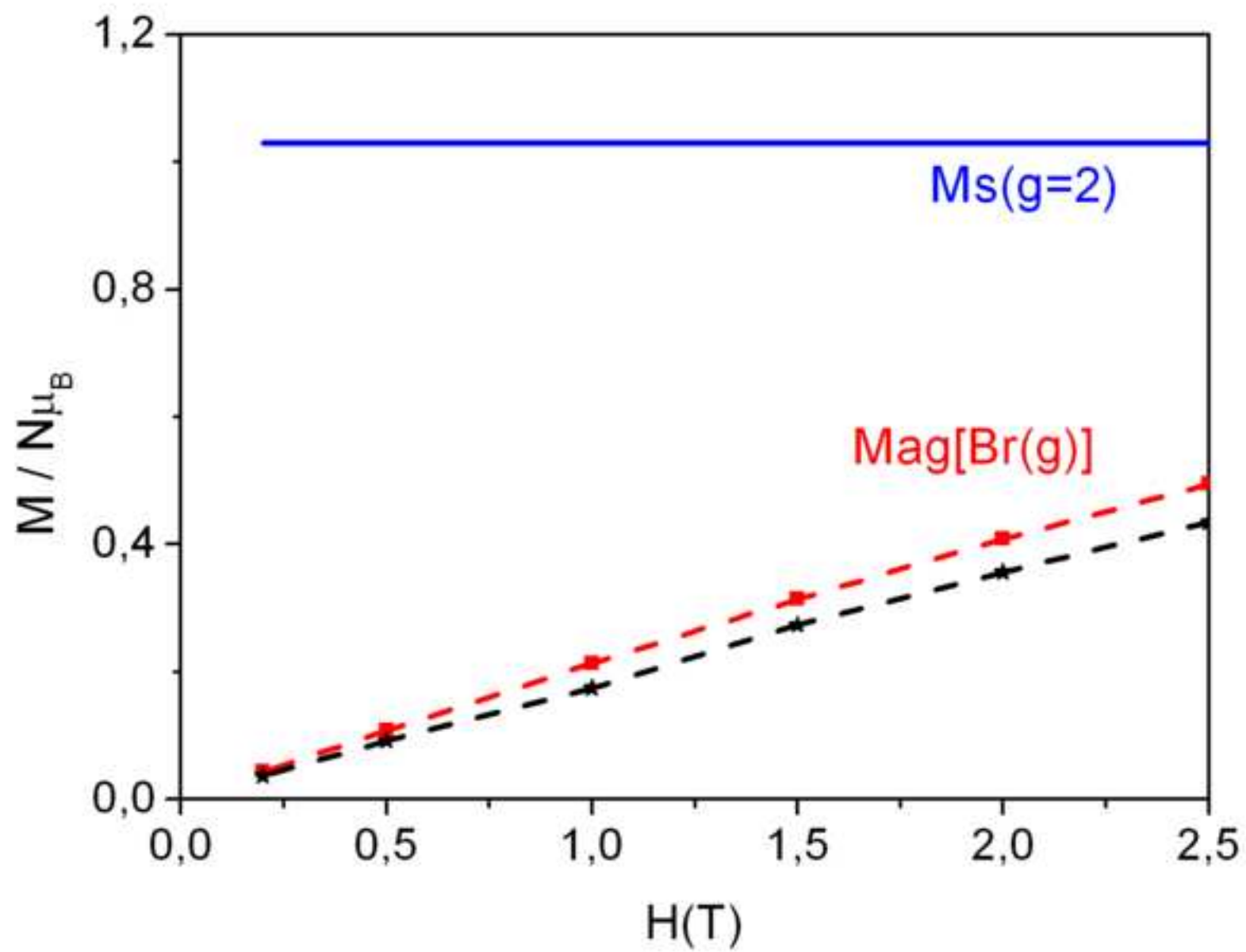


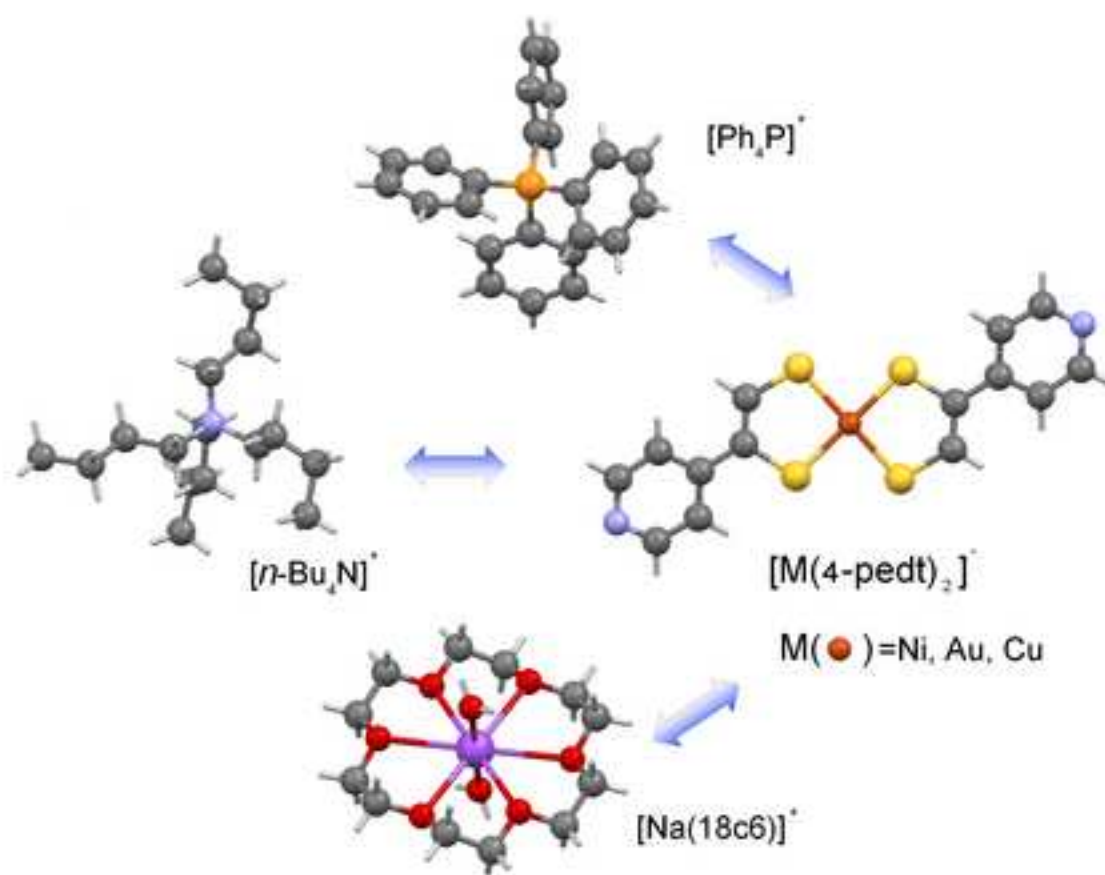












1 **Graphical Abstract**

2

3 The synthesis of $M(4\text{-pedt})_2$ complexes of nickel, copper and gold obtained as
4 tetrabutylammonium, tetraphenylphosphonium or sodium 18-crown-6 ether salts are
5 described and these compounds are characterised by single-crystal X-ray diffraction, cyclic
6 voltammetry, EPR and magnetic susceptibility measurements.

7

8

9

10